

**OFFICE OF CIVILIAN RADIOACTIVE WASTE MANAGEMENT
DESIGN CALCULATION OR ANALYSIS COVER SHEET**

1. QA: QA
2. Page 1

3. System: Uncanistered Spent Nuclear Fuel	4. Document Identifier: 000-00C-DSU0-00800-000-00A	5. Verified: <input type="checkbox"/> Yes <input checked="" type="checkbox"/> No
---	---	---

6. Title:
Vertical Drop of 44-BWR Waste Package with Lifting Collars

7. Group:
Analyses & Component Design, Structural Design

8. Document Status Designation:

Preliminary Final Superseded Cancelled

9.

T F

1. This product contains no potentially sensitive information.
 2. This product contains information that could define a target.
 3. This product contains information that could define a specific location.
 4. This product contains information that identifies vulnerabilities.

10. Notes/Comments:

None.

**NOTICE OF OPEN CHANGE DOCUMENTS - THIS DOCUMENT
IS IMPACTED BY THE LISTED CHANGE DOCUMENTS AND
CANNOT BE USED WITHOUT THEM.**

1) ECN-001, DATED 08/26/2005

+

Attachments		Total Number of Pages
Attachment I on Compact Disc		N/A
Attachment II - Sketch SK-0220 REV 01		4
Attachment III - Sketch SK-0234 REV 01		5

RECORD OF REVISIONS								
11. No.	12. Reason for Revision	13. Total No. of Pages	14. Last Page No.	15. Originator (Print/Sign)	16. Checker (Print/Sign)	17. Quality Engineering Representative (Print/Sign)	18. Approved/ Accepted (Print/Sign)	19. Date
A	Initial Issuance.	40	III-5	Adam K. Scheider <i>Adam K. Scheider</i>	Valerie de la Brosse <i>V. de la Brosse</i>	Dan Tunney <i>D. Tunney</i> 10/4/2002	M. J. ANDERS <i>M. J. ANDERS</i> 10/4/2002	10/4/02

CONTENTS

	Page
1. PURPOSE	4
2. METHOD	4
3. ASSUMPTIONS.....	4
4. USE OF COMPUTER SOFTWARE.....	6
5. CALCULATION	7
5.1 MASS AND GEOMETRIC DIMENSIONS OF WASTE PACKAGE	7
5.2 MATERIAL PROPERTIES.....	7
5.2.1 Calculations for Elevated-Temperature Material Properties.....	10
5.2.2 Calculations for True Measures of Ductility.....	10
5.2.3 Calculations for Tangent Moduli	13
5.3 INITIAL VELOCITY OF WASTE PACKAGE.....	15
5.4 FINITE ELEMENT REPRESENTATION.....	16
6. RESULTS	17
7. REFERENCES	29
8. ATTACHMENTS.....	31

FIGURES

	Page
Figure 5-1. Vertical Drop Geometry.....	15
Figure 6-1. Outer Shell at Room Temperature (Pa).....	18
Figure 6-2. Inner Shell at Room Temperature (Pa).....	19
Figure 6-3. Outer Shell Refined Mesh at Room Temperature (Pa)	20
Figure 6-4. Inner Shell Refined Mesh at Room Temperature (Pa)	21
Figure 6-5. Outer Shell at 400 °F (Pa)	22
Figure 6-6. Inner Shell at 400 °F (Pa)	23
Figure 6-7. Outer Shell at 600 °F (Pa)	24
Figure 6-8. Inner Shell at 600 °F (Pa)	25
Figure 6-9. Outer Shell at 600 °F with Vendor Elongation (Pa).....	26
Figure 6-10. Inner Shell at 600 °F with Vendor Elongation (Pa)	27

TABLES

	Page
Table 6-1. Mesh Verification.....	21
Table 6-2. Maximum Stress by Load Case.	28
Table 8-1. List of Files Submitted in the Form of Electronic Files in Attachment I	31

1. PURPOSE

The objective of this calculation is to determine the structural response of a waste package (WP) dropped flat on its bottom from a specified height. The WP used for that purpose is the 44-Boiling Water Reactor (BWR) WP. The scope of this document is limited to reporting the calculation results in terms of stress intensities. The Uncanistered Waste Disposal Container System is classified as Quality Level 1 (Ref. 4, page 7). Therefore, this calculation is subject to the requirements of the Quality Assurance Requirements and Description (Ref. 16). AP-3.12Q, *Design Calculations and Analyses* (Ref. 11) is used to perform the calculation and develop the document. The information provided by the sketches attached to this calculation is that of the potential design of the type of 44-BWR WP considered in this calculation and provides the potential dimensions and materials for that design.

2. METHOD

The finite element calculation was performed by using the commercially available LS-DYNA V950 (Software Tracking Number [STN] 10300-950-00; Ref. 7) finite element code. The results of this calculation were provided in terms of maximum stress intensities in the Outer Shell (OS) and Inner Shell (IS).

The control of electronic management of data was conducted in accordance with AP-3.13Q, *Design Control* (Ref. 19).

3. ASSUMPTIONS

In the course of developing this document, the following assumptions are made regarding the structural calculation. These assumptions do not require confirmation.

- 3.1 Some of the temperature-dependent material properties are not available for SB-575 N06022 (Alloy C-22), SA-516 K02700 (516 carbon steel [CS]), SA-240 S31600 (316 stainless steel [SS]), SA-240 S30400 SS (304 SS), and SA-705 S017400 (17-4 PH). The room-temperature (RT [70 °F]) density, Poisson's Ratio, and elongation are assumed for these materials. The impact of using room-temperature material properties is anticipated to be small. The rationale for this assumption is that undetermined mechanical properties of said materials will not significantly impact the results. This assumption is used in Section 5.2 and corresponds to paragraph 5.2.8.4 of Ref. 20.
- 3.2 The Poisson's ratio of Alloy C-22 is not available in literature. The Poisson's ratio of Alloy 625 (SB-443 N06625) is assumed for Alloy C-22. The impact of this assumption is anticipated to be negligible. The rationale for this assumption is that the chemical compositions of Alloy C-22 and Alloy 625 are similar (see Ref. 2, Section II, SB-575, Table 1 and Ref. 13, p. 143, respectively). This assumption is used in Section 5.2 and corresponds to paragraph 5.2.8.2 of Ref. 20.

3.3 Some of the rate-dependent material properties are not available for Alloy C-22, 316 CS, 316 SS, 17-4 PH, and 304 SS, and therefore will not be considered. The rationale for this assumption is that not taking strain-rate dependent material properties into account will yield conservative results. This assumption is used in Sections 5.2 and 5.3 and corresponds to paragraph 5.2.5 in Ref. 20.

3.4 The uniform strain of 304 SS is not available in literature. Therefore, it is assumed that the uniform strain is 75% of the elongation. The rationale for this assumption is the character of the stress-strain curve for 304 SS (Ref. 8, page 295). This assumption is used in Section 5.2.2 and corresponds to paragraph 5.2.14.1 of Ref. 20.

3.5 The exact geometry of the loaded internals was simplified for the purpose of this calculation. The fuel basket was represented using shell elements of a constant thickness. The individual fuel assemblies were represented as solid rectangles made from SA-240 S30400 (304 SS) and given an appropriate density to approximate the correct total mass. The rationale for this assumption was to simplify the finite element representation (FER) while preserving the pertinent physics of the problem. This assumption was used in Sections 5.2 and 5.4 and corresponds to paragraphs 5.2.9.1 and 5.2.9.2 of Ref. 20.

3.6 Three-stage deformation characteristics are not observed in the stress-strain curves for Alloy C-22 or 316 SS (Ref. 12). Therefore, it is conservatively assumed that the uniform strain is 90% of the elongation. The rationale for this assumption is the character of the stress-strain curves for Alloy C-22 and 316 SS. This assumption is used in Section 5.2.2 and corresponds to paragraph 5.2.8.6 of Ref. 20.

3.7 The Poisson's Ratio for 17-4 PH in the H900 condition is not available from traditional sources. It is assumed that this value is 0.272. The rationale for this assumption is that this is what is available from vendor resources (Ref. 17). The impact of this assumption is anticipated to be negligible. This assumption is used in Section 5.2.

3.8 It is assumed that the Engineering Stress and Engineering Strain will be representative of the True Stress and True Strain for 17-4 PH in the H900 condition. The rationale for this assumption is that this material is extremely hard in relation to the other metals being used. H900 is the hardest condition for which 17-4 PH is available. The elongation equals 10 % (Ref. 2, Section II, SA-705/SA-705M, Table 3) and the yield strength is very close to its ultimate strength. This assumption is used in Section 5.2.3.

3.9 The impact volume for the falling WP is assumed to be unyielding. The rationale for this assumption is that it maximizes the stress on the falling WP. This assumption is used in Section 5.2 and Section 5.4 and corresponds to paragraph 5.2.8.1 of Ref. 20.

3.10 The elongations of Alloy C-22 and 316 SS at elevated temperatures are not available from traditional sources. However, vendor data is available (Ref. 6, page 15 and Ref. 18, page 8).

The percent difference between elongations at RT and elevated temperatures can be normalized and applied to the data available from accepted codes. The rationale for this assumption is that the relative change of typical elongations should be bounding for the relative change of minimum elongation. Even though the values are not from traditional sources, the values are conservative and create higher stress intensities for the same temperature. This assumption is used in Section 5.2.1 and corresponds to paragraph 5.2.8.5 of Ref. 20.

3.11 The uniform strain of SA-516 K02700 carbon steel is not available in literature. Therefore, it is assumed that the uniform strain is 50% of the elongation. The rationale for this assumption is the character of the stress-strain curve for SA-36 carbon steel (Ref. 8, page 189) which has a similar chemical composition as SA-516 K02700 carbon steel (Ref. 2, Section II, SA-516/SA-516M, Table 1 and SA-36/SA-36M, Table 2). This assumption is used in Section 5.2.2 and corresponds to paragraph 5.2.11.1 of Ref. 20.

4. USE OF COMPUTER SOFTWARE

The qualified Finite Element Analysis (FEA) code used for this calculation is Livermore Software Technology Corporation (LSTC) LS-DYNA V950 (Ref. 7), which was obtained from the Software Configuration Management in accordance with appropriate procedures, and is identified by the Software Tracking Number 10300-950-00. LS-DYNA is a qualified, commercially available finite element code and is appropriate for structural calculations of waste packages as performed in this calculation. The calculations using LS-DYNA V950 were executed on the HP 9000 series UNIX workstations (operating system HP-UX B.10.20) identified with YMP tag numbers 114434 and 117162, located in Las Vegas, NV. The LS-DYNA evaluations performed for this calculation are fully within the range of the validation performed for the LS-DYNA V950 code. Access to the code was granted by the Software Configuration Management in accordance with the appropriate procedures.

TrueGrid, Version 2.1 was used in this calculation solely to mesh the geometric representations of the domain. The suitability and adequacy of this mesh is based on visual examination, engineering judgment, and the results of mesh verification in Section 6 (see Table 6-1). The mesh has been evaluated in accordance with AP-3.12Q (Ref. 11), and determined to be suitable and adequate for use as input to LS-DYNA V950. Therefore, the use of TrueGrid Version 2.1 is exempt from the requirements of AP-SI.1Q (Ref. 9, Section 2.1).

The input and output files are listed in Section 8 of this document. They are located in Attachment I to this document.

5. CALCULATION

5.1 MASS AND GEOMETRIC DIMENSIONS OF WASTE PACKAGE

This calculation was performed using mass and geometric dimensions of the 44-BWR Waste Package (see pp. II-2, II-3, III-1, III-2, III-4, and III-5):

Total mass of the loaded WP = 42,100 kg

Length = 5.097 m

Outer diameter of outer shell = 1.614 m

Outer diameter of lifting collar = 1.878 m

Total mass of the loaded WP and lifting collars = 45,100 kg

5.2 MATERIAL PROPERTIES

Material properties used in these calculations are listed in this section. Some of the temperature-dependent and rate-dependent material properties are not available for Alloy C-22, 316 SS, 17-4 PH, 516 CS and 304 SS. Therefore, RT density and Poisson's ratio obtained under the static loading conditions are used for all materials (see Assumptions 3.1 and 3.3). Furthermore, all material properties listed below are obtained under static loading conditions (see Assumption 3.3).

SB-575 N06022 (Alloy C-22) (Outer shell, outer shell lids, support ring, upper and lower trunnion collar sleeves):

- Density = 8690 kg/m³ (0.314 lb/in³) (at RT) (Ref. 2, Section II, SB-575 Section 7.1)
- Yield strength = 310 MPa (45 ksi) (at RT) (Ref. 2, Section II, Table Y-1)
Yield strength = 236 MPa (34.3 ksi) (at 400 °F = 204 °C) (Ref. 2, Section II, Table Y-1)
Yield strength = 211 MPa (30.6 ksi) (at 600 °F = 316 °C) (Ref. 2, Section II, Table Y-1)
- Tensile strength = 689 MPa (100 ksi) (at RT) (Ref. 2, Section II, Table U)
Tensile strength = 657 MPa (95.3 ksi) (at 400 °F = 204 °C) (Ref. 2, Section II, Table U)
Tensile strength = 628 MPa (91.1 ksi) (at 600 °F = 316 °C) (Ref. 2, Section II, Table U)
- Elongation = 0.45 (at RT) (Ref. 2, Section II, SB-575 Table 3)
- Poisson's ratio = 0.278 (at RT) (Ref. 13, p. 143; see Assumption 3.2)
- Modulus of elasticity = 206 GPa (at RT) (Ref. 6, p. 14)
Modulus of elasticity = 196 GPa (at 400 °F = 204 °C) (Ref. 6, p. 14)
Modulus of elasticity = 190 GPa (at 600 °F = 316 °C) (Ref. 6, p. 14)

SA-240 S31600 (316 SS) (Inner shell, inner shell lids, interface ring, and shear ring):

- Density = 7980 kg/m^3 (at RT) (Ref. 14, Table X1.1, p. 7)
- Yield strength = 207 MPa (30.0 ksi) (at RT) (Ref. 2, Section II, Table Y-1)
Yield strength = 148 MPa (21.4 ksi) (at $400^\circ\text{F} = 204^\circ\text{C}$) (Ref. 2, Section II, Table Y-1)
Yield strength = 130 MPa (18.9 ksi) (at $600^\circ\text{F} = 316^\circ\text{C}$) (Ref. 2, Section II, Table Y-1)
- Tensile strength = 517 MPa (75.0 ksi) (at RT) (Ref. 2, Section II, Table U)
Tensile strength = 496 MPa (71.9 ksi) (at $400^\circ\text{F} = 204^\circ\text{C}$) (Ref. 2, Section II, Table U)
Tensile strength = 495 MPa (71.8 ksi) (at $600^\circ\text{F} = 316^\circ\text{C}$) (Ref. 2, Section II, Table U)
- Elongation = 0.40 (at RT) (Ref. 2, Section II, SA-240 Table 2)
- Poisson's ratio = 0.30 (at RT) (Ref. 13, Figure 15, p. 755)
- Modulus of elasticity = 195 GPa ($28.3 \times 10^6 \text{ psi}$) (at RT) (Ref. 2, Section II, Table TM-1)
Modulus of elasticity = 183 GPa ($26.5 \times 10^6 \text{ psi}$) (at $400^\circ\text{F} = 204^\circ\text{C}$) (Ref. 2, Section II, Table TM-1)
Modulus of elasticity = 174 GPa ($25.3 \times 10^6 \text{ psi}$) (at $600^\circ\text{F} = 316^\circ\text{C}$) (Ref. 2, Section II, Table TM-1)

SA-240 S30400 (304 SS) (44-BWR Fuel Assemblies, see Assumption 3.5):

- Yield strength = 207 MPa (30.0 ksi) (at RT) (Ref. 2, Section II, Table Y-1)
Yield strength = 143 MPa (20.7 ksi) (at $400^\circ\text{F} = 204^\circ\text{C}$) (Ref. 2, Section II, Table Y-1)
Yield strength = 127 MPa (18.4 ksi) (at $600^\circ\text{F} = 316^\circ\text{C}$) (Ref. 2, Section II, Table Y-1)
- Tensile strength = 517 MPa (75.0 ksi) (at RT) (Ref. 2, Section II, Table U)
Tensile strength = 441 MPa (64.0 ksi) (at $400^\circ\text{F} = 204^\circ\text{C}$) (Ref. 2, Section II, Table U)
Tensile strength = 437 MPa (63.4 ksi) (at $600^\circ\text{F} = 316^\circ\text{C}$) (Ref. 2, Section II, Table U)
- Elongation = 0.40 (at RT) (Ref. 2, Section II, SA-240 Table 2)
- Poisson's ratio = 0.29 (at RT) (Ref. 13, Figure 15, p. 755)
- Modulus of elasticity = 195 GPa ($28.3 \times 10^6 \text{ psi}$) (at RT) (Ref. 2, Section II, Table TM-1)
Modulus of elasticity = 183 GPa ($26.5 \times 10^6 \text{ psi}$) (at $400^\circ\text{F} = 204^\circ\text{C}$) (Ref. 2, Section II, Table TM-1)
Modulus of elasticity = 174 GPa ($25.3 \times 10^6 \text{ psi}$) (at $600^\circ\text{F} = 316^\circ\text{C}$) (Ref. 2, Section II, Table TM-1)

SA-36/36M K02600 (A36 CS, see Assumptions 3.9) (Impact Volume):

- Density = 7860 kg/m^3 (at RT) (Ref. 14, Table X1.1, p. 7)
- Poisson's ratio = 0.30 (at RT) (Ref. 3, p. 374)
- Modulus of elasticity = 203 GPa ($29.5 * 10^6 \text{ psi}$) (at RT) (Ref. 2, Section II, Table TM-1)

SA-705 S17400 (17-4 PH [H900 Condition]) (Lifting Collars):

- Density = 7800 kg/m^3 (at RT) (Ref. 13, Table 12, page 34)
- Yield strength = 1170 MPa (170 ksi) (at RT) (Ref. 5, page 506)
Yield strength = 1030 MPa (150 ksi) (at $400^\circ\text{F} = 204^\circ\text{C}$) (Ref. 5, page 506)
Yield strength = 965 MPa (140 ksi) (at $600^\circ\text{F} = 316^\circ\text{C}$) (Ref. 5, page 506)
- Tensile strength = 1310 MPa (190 ksi) (at RT) (Ref. 5, page 506)
Tensile strength = 1190 MPa (173 ksi) (at $400^\circ\text{F} = 204^\circ\text{C}$) (Ref. 5, page 506)
Tensile strength = 1100 MPa (160 ksi) (at $600^\circ\text{F} = 316^\circ\text{C}$) (Ref. 5, page 506)
- Elongation = 0.10 (at RT) (Ref. 2, Section II, SA-705/SA-705M, Table 3)
- Poisson's ratio = 0.272 (at RT) (Ref. 17, Table "Physical Properties", see Assumption 3.7)
- Modulus of elasticity = 197 GPa ($28.5 * 10^6 \text{ psi}$) (at RT) (Ref. 2, Section II, Table TM-1)
Modulus of elasticity = 183 GPa ($26.6 * 10^6 \text{ psi}$) (at $400^\circ\text{F} = 204^\circ\text{C}$) (Ref. 2, Section II, Table TM-1)
Modulus of elasticity = 176 GPa ($25.5 * 10^6 \text{ psi}$) (at $600^\circ\text{F} = 316^\circ\text{C}$) (Ref. 2, Section II, Table TM-1)

SA-516 K02700 (516 CS) (Sideguides, stiffeners, and baskets):

- Density = 7850 kg/m^3 (at RT) (Ref. 2, SA-20/SA20M, Section 14.1)
- Yield strength = 262 MPa (38 ksi) (at RT) (Ref. 2, Section II, Table Y-1)
Yield strength = 224 MPa (32.5 ksi) (at $400^\circ\text{F} = 204^\circ\text{C}$) (Ref. 2, Section II, Table Y-1)
Yield strength = 201 MPa (29.1 ksi) (at $600^\circ\text{F} = 316^\circ\text{C}$) (Ref. 2, Section II, Table Y-1)
- Tensile strength = 483 MPa (70 ksi) (at RT) (Ref. 2, Section II, Table U)
Tensile strength = 483 MPa (70 ksi) (at $400^\circ\text{F} = 204^\circ\text{C}$) (Ref. 2, Section II, Table U)
Tensile strength = 483 MPa (70 ksi) (at $600^\circ\text{F} = 316^\circ\text{C}$) (Ref. 2, Section II, Table U)

- Elongation = 0.21 (at RT) (Ref. 2, Section II, SA-516/SA-516M, Table 2)
- Poisson's ratio = 0.3 (at RT) (Ref. 3, p. 374)
- Modulus of elasticity = 203 GPa ($29.5 * 10^6 \text{ psi}$) (at RT) (Ref. 2, Section II, Table TM-1)
 Modulus of elasticity = 191 GPa ($27.7 * 10^6 \text{ psi}$) (at $400 \text{ }^{\circ}\text{F} = 204 \text{ }^{\circ}\text{C}$) (Ref. 2, Section II, Table TM-1)
 Modulus of elasticity = 184 GPa ($26.7 * 10^6 \text{ psi}$) (at $600 \text{ }^{\circ}\text{F} = 316 \text{ }^{\circ}\text{C}$) (Ref. 2, Section II, Table TM-1)

5.2.1 Calculations for Elevated-Temperature Material Properties

The values for elongation at elevated temperatures are not listed in conventional listings such as American Society for Testing and Materials (ASTM) Standards or American Society of Mechanical Engineers (ASME) Boiler and Pressure Vessel Code. However, the elongation values at elevated temperatures are available from vendor data. This vendor data will be used to estimate elevated temperature elongations normalized to the RT values from accepted codes (see Assumption 3.10).

For Alloy C-22, the vendor data shows a 10% increase between RT and $600 \text{ }^{\circ}\text{F}$ (Ref. 6, page 15). Therefore the elongation value for Alloy C-22 at $600 \text{ }^{\circ}\text{F}$ will be as follows:

$$\text{Elongation}_{600 \text{ }^{\circ}\text{F}} = 0.45 * 1.10 = 0.50$$

For 316 SS, the vendor data shows a 30% decrease between RT and $600 \text{ }^{\circ}\text{F}$ (Ref. 18, page 3). Therefore the elongation value for 316 SS at $600 \text{ }^{\circ}\text{F}$ will be as follows:

$$\text{Elongation}_{600 \text{ }^{\circ}\text{F}} = 0.40 * (1 - 0.30) = 0.28$$

Since the components made of 516 CS, 17-4 PH, and 304 SS will not be analyzed for stresses, their elongations are not needed at elevated temperatures.

5.2.2 Calculations for True Measures of Ductility

The material properties in Sections 5.1 and 5.2 refer to engineering stress and strain definitions:

$$s = \frac{P}{A_0} \text{ and } e = \frac{L - L_0}{L_0} \quad (\text{Ref. 10, Chapter 9})$$

Where P stands for the force applied during static tensile test, L is the deformed-specimen length, and L_0 and A_0 are original length and cross-sectional area of specimen, respectively. It is generally accepted that the engineering stress-strain curve does not give a true indication of the deformation characteristics of a material during the plastic deformation since it is based entirely on the original

dimensions of the specimen. Therefore, the LS-DYNA V950 finite element code requires input in terms of true stress and strain definitions. These definitions are:

$$\sigma = \frac{P}{A} \text{ and } \varepsilon = \ln\left(\frac{L}{L_0}\right) \quad (\text{Ref. 10, Chapter 9})$$

The relationships between the true stress and strain definitions and engineering stress and strain definitions can be readily derived based on constancy of volume ($A_0 \cdot L_0 = A \cdot L$) and strain homogeneity during plastic deformation:

$$\sigma = s \cdot (1 + e) \text{ and } \varepsilon = \ln(1 + e) \quad (\text{Ref. 10, Chapter 9})$$

These expressions are applicable only in the hardening region of stress-strain curve that is limited by the onset of necking.

The following parameters are used in the subsequent calculations:

$s_y \approx \sigma_y$ \equiv yield strength

$s_u \equiv$ engineering tensile strength

$\sigma_u \equiv$ true tensile strength

$e_y \approx \varepsilon_y$ \equiv strain corresponding to yield strength

$e_u \equiv$ engineering strain corresponding to tensile strength (engineering uniform strain)

$\varepsilon_u \equiv$ true strain corresponding to tensile strength (true uniform strain)

In absence of the uniform strain data in available literature, it needs to be estimated based on stress-strains curves and elongation (strain corresponding to rupture of the tensile specimen).

The stress-strain curves for Alloy C-22 and 316 SS do not manifest three-stage deformation character (Ref. 12). Therefore, the elongation, reduced by 10% for the sake of conservatism, can be used in place of uniform strain (Assumption 3.6).

In the case of Alloy C-22 ($e_u = 0.9 * \text{elongation} = 0.41$ at RT), the true measures of ductility are

$$\varepsilon_u = \ln(1 + e_u) = \ln(1 + 0.41) = 0.34$$

$$\sigma_u = s_u * (1 + e_u) = 689 * (1 + 0.41) = 971 \text{ MPa.}$$

400 °F (204 °C) Alloy C-22

$$\varepsilon_u = \ln(1 + e_u) = \ln(1 + 0.41) = 0.34$$

$$\sigma_u = s_u * (1 + e_u) = 657 * (1 + 0.41) = 926 \text{ MPa}$$

600 °F (316 °C) Alloy C-22

$$\varepsilon_u = \ln(1 + e_u) = \ln(1 + 0.41) = 0.34$$

(ASME values)

$$\sigma_u = s_u * (1 + e_u) = 628 * (1 + 0.41) = 885 \text{ MPa}$$

(ASME values)

$$\varepsilon_u = \ln(1 + e_u) = \ln(1 + 0.45) = 0.37$$

(vendor data)

$$\sigma_u = s_u * (1 + e_u) = 628 * (1 + 0.45) = 911 \text{ MPa}$$

(vendor data)

For 316 SS at RT, $e_u = 0.9 * \text{elongation} = 0.36$, therefore:

$$\varepsilon_u = \ln(1 + e_u) = \ln(1 + 0.36) = 0.31$$

$$\sigma_u = s_u * (1 + e_u) = 517 * (1 + 0.36) = 703 \text{ MPa}$$

400 °F (204 °C) 316 SS

$$\varepsilon_u = \ln(1 + e_u) = \ln(1 + 0.36) = 0.31$$

$$\sigma_u = s_u * (1 + e_u) = 496 * (1 + 0.36) = 675 \text{ MPa}$$

600 °F (316 °C) 316 SS

$$\varepsilon_u = \ln(1 + e_u) = \ln(1 + 0.36) = 0.31$$

(ASME values)

$$\sigma_u = s_u * (1 + e_u) = 495 * (1 + 0.36) = 673 \text{ MPa}$$

(ASME values)

$$\varepsilon_u = \ln(1 + e_u) = \ln(1 + 0.25) = 0.22$$

(vendor data)

$$\sigma_u = s_u * (1 + e_u) = 495 * (1 + 0.25) = 619 \text{ MPa}$$

(vendor data)

For 516 CS at RT, $e_u = 0.5 * \text{elongation} = 0.11$ (see Assumption 3.11), therefore:

$$\varepsilon_u = \ln(1 + e_u) = \ln(1 + 0.11) = 0.10$$

$$\sigma_u = s_u * (1 + e_u) = 483 * (1 + 0.11) = 536 \text{ MPa}$$

400 °F (204 °C) 516 CS

$$\varepsilon_u = \ln(1 + e_u) = \ln(1 + 0.11) = 0.10$$

$$\sigma_u = s_u * (1 + e_u) = 483 * (1 + 0.11) = 536 \text{ MPa}$$

600 °F (316 °C) 516 CS

$$\varepsilon_u = \ln(1 + e_u) = \ln(1 + 0.11) = 0.10$$

$$\sigma_u = s_u * (1 + e_u) = 483 * (1 + 0.11) = 536 \text{ MPa}$$

For 304 SS at RT, $e_u = 0.75 * \text{elongation} = 0.30$ (see Assumption 3.4), therefore:

$$\varepsilon_u = \ln(1 + e_u) = \ln(1 + 0.30) = 0.26$$

$$\sigma_u = s_u * (1 + e_u) = 517 * (1 + 0.30) = 672 \text{ MPa}$$

400 °F (204 °C) 304 SS

$$\varepsilon_u = \ln(1 + e_u) = \ln(1 + 0.30) = 0.26$$

$$\sigma_u = s_u * (1 + e_u) = 441 * (1 + 0.30) = 573 \text{ MPa}$$

600 °F (316 °C) 304 SS

$$\varepsilon_u = \ln(1 + e_u) = \ln(1 + 0.30) = 0.26$$

$$\sigma_u = s_u * (1 + e_u) = 437 * (1 + 0.30) = 568 \text{ MPa}$$

5.2.3 Calculations for Tangent Moduli

As previously discussed, the results of this simulation are required to include elastic and plastic deformations for Alloy C-22, 516 CS, 304 SS, 17-4 PH, and 316 SS. When the materials are driven into the plastic range, the slope of the stress-strain curves continuously changes. Thus, a simplification for these curves is needed to incorporate plasticity into the FER. A standard approximation commonly used in engineering is to use a straight line that connects the yield point and the tensile strength point of the material. The parameters used in the subsequent calculations in addition to those defined in Section 5.1.2 are modulus of elasticity (E) and tangent modulus (E_t). The tangent (hardening) modulus represents the slope of the stress-strain curve in the plastic region. In the case of Alloy C-22, the strain corresponding to the yield strength is:

$$\varepsilon_{y,n} = \sigma_y/E = 310 * 10^6 / 206 * 10^9 = 0.0015 \text{ (see Section 5.2.1)}$$

Hence, the tangent modulus at RT is:

$$E_{t,n} = (\sigma_{u,n} - \sigma_{y,n}) / (\varepsilon_{u,n} - \varepsilon_{y,n}) = (0.973 - 0.310)/(0.34 - 0.0015) = 2.0 \text{ GPa} \text{ (see Section 5.2, 5.2.1, and 5.2.2)}$$

For Alloy C-22 at 400 °F (204 °C)

$$E_{t,400^\circ F} = (\sigma_{u,400^\circ F} - \sigma_{y,400^\circ F}) / (\varepsilon_{u,400^\circ F} - \sigma_{y,400^\circ F}/E_{400^\circ F}) = (0.926 - 0.236)/(0.34 - 236/196e3) = 2.0 \text{ GPa} \text{ (see Section 5.2, 5.2.1, and 5.2.2)}$$

For Alloy C-22 at 600 °F (316 °C, ASME values)

$$E_{t,600^\circ F} = (\sigma_{u,600^\circ F} - \sigma_{y,600^\circ F}) / (\varepsilon_{u,600^\circ F} - \sigma_{y,600^\circ F}/E_{600^\circ F}) = (0.885 - 0.211)/(0.34 - 211/190e3) = 2.0 \text{ GPa} \text{ (see Section 5.2, 5.2.1, and 5.2.2)}$$

For Alloy C-22 at 600 °F (316 °C, vendor data)

$$E_{t,600^\circ F} = (\sigma_{u,600^\circ F} - \sigma_{y,600^\circ F}) / (\varepsilon_{u,600^\circ F} - \sigma_{y,600^\circ F}/E_{600^\circ F}) = (0.911 - 0.211)/(0.37 - 211/190e3) = 1.9 \text{ GPa} \text{ (see Section 5.2, 5.2.1, and 5.2.2)}$$

Similarly, for 316 SS at RT:

$$E_{t,n} = (\sigma_{u,n} - \sigma_{y,n}) / (\varepsilon_{u,n} - \sigma_{y,n}/E_n) = (0.703 - 0.207)/(0.31 - 207/195e3) = 1.6 \text{ GPa} \text{ (see Section 5.2, 5.2.1, and 5.2.2)}$$

For 316 SS at 400 °F (204 °C)

$E_{t,400^\circ F} = (\sigma_{u,400^\circ F} - \sigma_{y,400^\circ F}) / (\varepsilon_{u,400^\circ F} - \sigma_{y,400^\circ F}/E_{400^\circ F}) = (0.675 - 0.148)/(0.31 - 148/183e3) = 1.7 \text{ GPa}$ (see Section 5.2, 5.2.1, and 5.2.2)

For 316 SS at 600 °F (316 °C, ASME values)

$E_{t,600^\circ F} = (\sigma_{u,600^\circ F} - \sigma_{y,600^\circ F}) / (\varepsilon_{u,600^\circ F} - \sigma_{y,600^\circ F}/E_{600^\circ F}) = (0.673 - 0.130)/(0.31 - 130/174e3) = 1.8 \text{ GPa}$ (see Section 5.2, 5.2.1, and 5.2.2)

For 316 SS at 600 °F (316 °C, vendor data)

$E_{t,600^\circ F} = (\sigma_{u,600^\circ F} - \sigma_{y,600^\circ F}) / (\varepsilon_{u,600^\circ F} - \sigma_{y,600^\circ F}/E_{600^\circ F}) = (0.619 - 0.130)/(0.22 - 130/174e3) = 2.2 \text{ GPa}$ (see Section 5.2, 5.2.1, and 5.2.2)

Tangent Modulus of 516 CS at RT:

$E_{t,r} = (\sigma_{u,r} - \sigma_{y,r}) / (\varepsilon_{u,r} - \sigma_{y,r}/E_r) = (0.536 - 0.262)/(0.10 - 262/203e3) = 2.8 \text{ GPa}$ (see Section 5.2, 5.2.1, and 5.2.2)

516 CS at 400 °F (204 °C)

$E_{t,400^\circ F} = (\sigma_{u,400^\circ F} - \sigma_{y,400^\circ F}) / (\varepsilon_{u,400^\circ F} - \sigma_{y,400^\circ F}/E_{400^\circ F}) = (0.536 - 0.224)/(0.10 - 224/191e3) = 3.2 \text{ GPa}$ (see Section 5.2, 5.2.1, and 5.2.2)

516 CS at 600 °F (316 °C)

$E_{t,600^\circ F} = (\sigma_{u,600^\circ F} - \sigma_{y,600^\circ F}) / (\varepsilon_{u,600^\circ F} - \sigma_{y,600^\circ F}/E_{600^\circ F}) = (0.536 - 0.201)/(0.10 - 201/184e3) = 3.4 \text{ GPa}$ (see Section 5.2, 5.2.1, and 5.2.2)

Tangent Modulus of 304 SS at RT:

$E_{t,r} = (\sigma_{u,r} - \sigma_{y,r}) / (\varepsilon_{u,r} - \sigma_{y,r}/E_r) = (0.672 - 0.207)/(0.26 - 207/195e3) = 1.8 \text{ GPa}$ (see Section 5.2, 5.2.1, and 5.2.2)

304 SS at 400 °F (204 °C)

$E_{t,400^\circ F} = (\sigma_{u,400^\circ F} - \sigma_{y,400^\circ F}) / (\varepsilon_{u,400^\circ F} - \sigma_{y,400^\circ F}/E_{400^\circ F}) = (0.573 - 0.143)/(0.26 - 143/183e3) = 1.7 \text{ GPa}$ (see Section 5.2, 5.2.1, and 5.2.2)

304 SS at 600 °F (316 °C)

$E_{t,600^\circ F} = (\sigma_{u,600^\circ F} - \sigma_{y,600^\circ F}) / (\varepsilon_{u,600^\circ F} - \sigma_{y,600^\circ F}/E_{600^\circ F}) = (0.568 - 0.127)/(0.26 - 127/174e3) = 1.7 \text{ GPa}$ (see Section 5.2, 5.2.1, and 5.2.2)

Tangent Modulus of 17-4 PH (H900 condition) at RT (see Assumption 3.8):

$E_{t,r} = (\sigma_{u,r} - \sigma_{y,r}) / (\varepsilon_{u,r} - \sigma_{y,r}/E_r) = (1.31 - 1.17)/(0.10 - 1170/197e3) = 1.5 \text{ GPa}$ (see Section 5.2, 5.2.1, and 5.2.2)

17-4 PH at 400 °F (204 °C)

$E_{t,400^\circ F} = (\sigma_{u,400^\circ F} - \sigma_{y,400^\circ F}) / (\varepsilon_{u,400^\circ F} - \sigma_{y,400^\circ F}/E_{400^\circ F}) = (1.19 - 1.03)/(0.10 - 1030/183e3) = 1.7 \text{ GPa}$ (see Section 5.2, 5.2.1, and 5.2.2)

17-4 PH at 600 °F (316 °C)

$$E_{1,600^{\circ}F} = (\sigma_{u,600^{\circ}F} - \sigma_{y,600^{\circ}F}) / (\varepsilon_{u,600^{\circ}F} - \varepsilon_{y,600^{\circ}F}) = (1.10 - 0.965) / (0.10 - 965/176e3) = 1.4 \text{ GPa} \text{ (see Section 5.2, 5.2.1, and 5.2.2)}$$
5.3 INITIAL VELOCITY OF WASTE PACKAGE

To reduce the computer execution time while preserving all features of the problem relevant to the structural calculation, the WP is set in a position just before impact and given an appropriate initial velocity as can be seen in Figure 5-1.

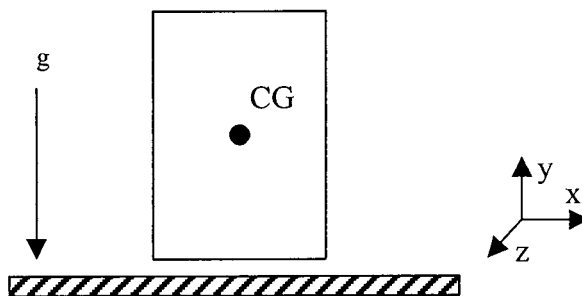


Figure 5-1. Vertical Drop Geometry

Using the following parameters:

$g \equiv$ acceleration due to gravity = 9.81 m/s^2

$S \equiv$ Drop Height = 2.0 m (Ref. 1, Section 1.2.2.1.3)

and Newton's equation of motion:

$$V^2 = V_0^2 + 2a(S - S_0)$$

Substituting values in yields:

$$V^2 = 0^2 + 2 * (9.81 \text{ m/s}^2) * (2.0 \text{ m}), \text{ which reduces to}$$

$$V = 6.26 \text{ m/s}$$

5.4 FINITE ELEMENT REPRESENTATION

A half-symmetry three-dimensional FER of the WP was developed in TrueGrid using the dimensions provided in Attachments II and III.

The internal structure of the WP was simplified. The internal components of the IS (fuel basket, thermal shunts, side guides, spent nuclear fuel, etc.) were simplified in the FER (Assumption 3.5). The thermal shunts (made from aluminum) were not included in the representation, which is conservative. It is conservative since including the plates would make the basket stronger. Not including the thermal shunts lowered the number of contacts within the FER while still maintaining the proper mass needed for the computer run.

The impact volume was conservatively assumed to be unyielding (Assumption 3.9). This was accomplished using a target surface made from A36 CS, a mild steel commonly used in construction. This impact volume was defined in LS-DYNA without plastic material properties. Therefore, by definition, it is an unyielding surface.

The mesh of the FER was appropriately generated and refined in the contact region according to standard engineering practice (see Table 6-1). Thus, the accuracy of the results of this calculation is deemed acceptable.

The initial drop height of the WP was reduced to a very small distance before impact and the WP was given an initial velocity equal to 6.26 m/s (see Section 5.3).

The FER was then used in LS-DYNA V950 to perform the transient dynamic analysis for the 44-BWR Waste Package vertical drop.

6. RESULTS

Attachment I includes the input files and results files that show execution of the programs occurred correctly. The stresses were recorded every 0.001 seconds after impact. The stresses in the OS and IS peaked between 0.004 and 0.013 seconds. However, the solution was allowed to reach 0.014 seconds to ensure that all stresses had climaxed.

The results file, d3hsp (Attachment I), lists the masses calculated by LS-DYNA. The total mass of the WP equals 48,500 kg, while the mass of the loaded WP is 45,100 kg from Section 5.1. The percent difference in mass is approximately 7.4%. However, it is conservative since the mass from LS-DYNA is more than that from Attachment II.

The following pages contain figures that show various parts at states of maximum stress. These start on the next page with Figure 6-1, which shows the maximum stress in the OS at RT. The stresses in the IS lid and the shear ring that holds the IS lid in place were not reported. Since the impact of the vertical drop occurs at the bottom of the WP, and the IS lid and shear ring are located at the top, these components did not sustain a significant amount of damage to justify reporting their stresses.

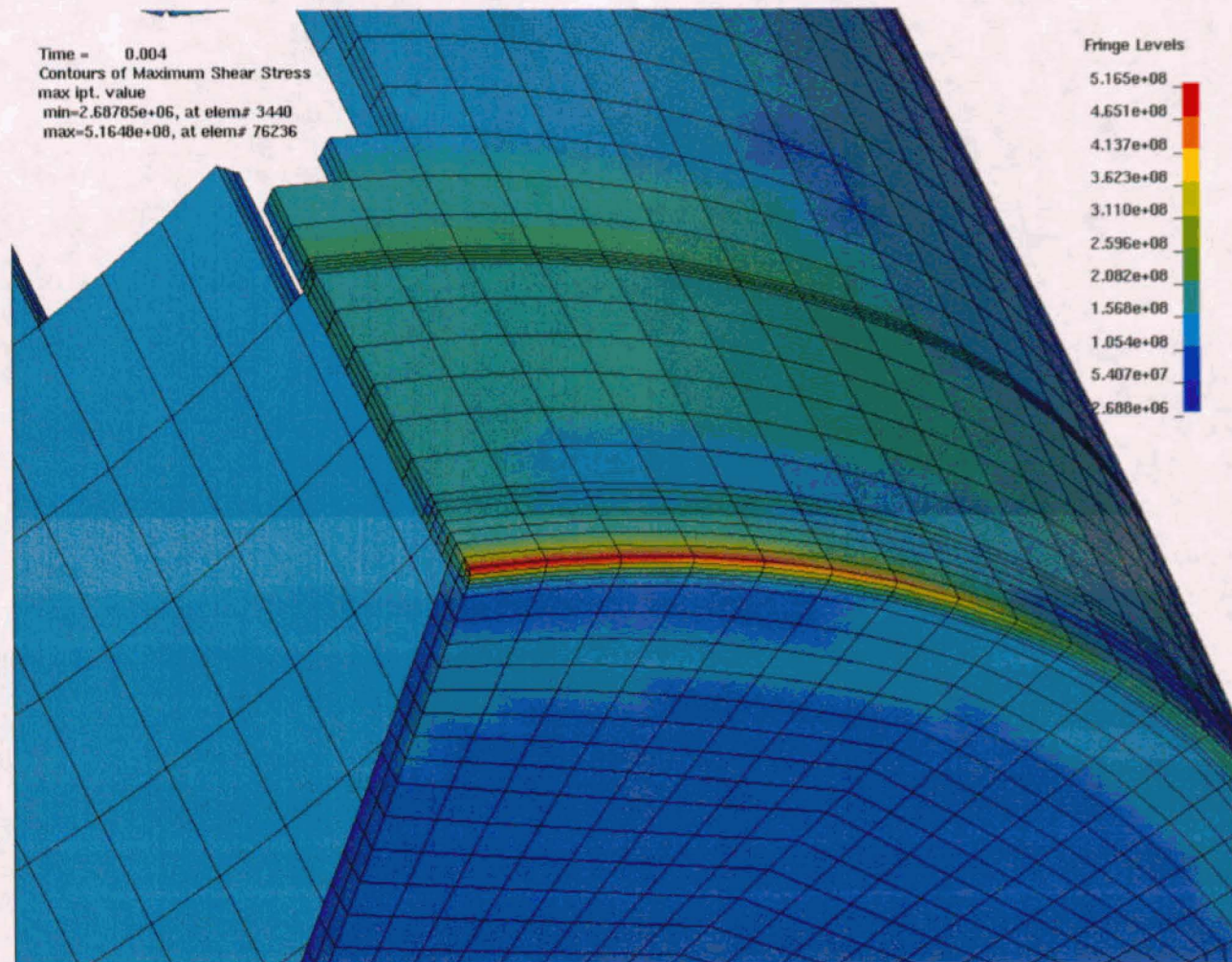


Figure 6-1. Outer Shell at Room Temperature (Pa)

All of the stresses that are reported in the legends of the plots are Tresca stresses or maximum shear stresses. The units are Pascals. Stress intensity is defined as twice the maximum shear stress. In order to report stress intensity, therefore, the maximum shear stress must be multiplied by 2. Figure 6-1 shows that the maximum stress intensity in the OS at RT is 1030 MPa at 0.004 seconds. By comparing the color of the mesh with that of the legend, it should be noted that this stress does not occur completely through the thickness of the OS.

Figure 6-2 may be found on the next page. It shows the maximum shear stress in the IS at RT.

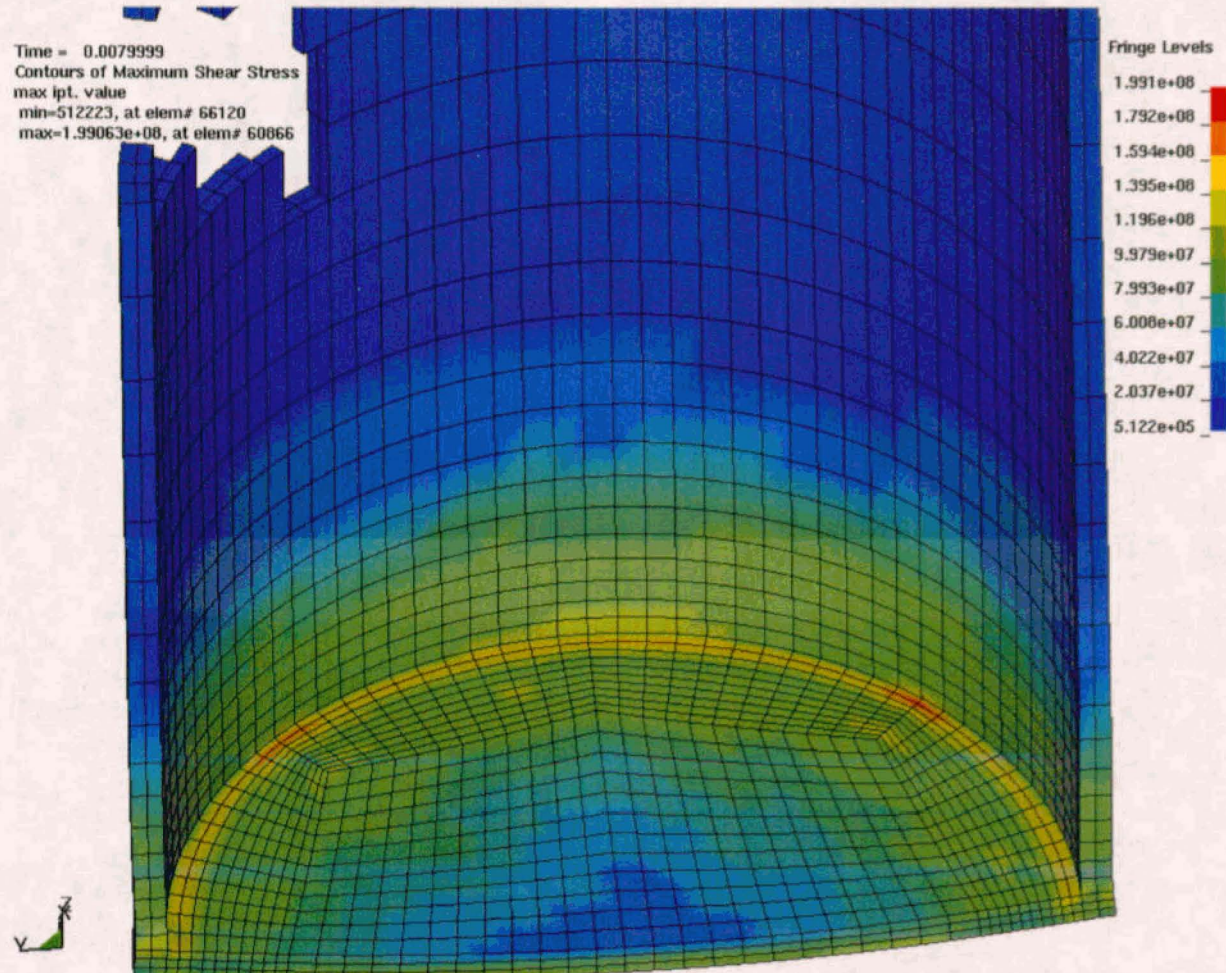


Figure 6-2. Inner Shell at Room Temperature (Pa)

Figure 6-2 shows that the maximum stress intensity in the IS is 398 MPa at 0.008 seconds. Figure 6-3 may be found on the next page. It shows the maximum shear stress in the OS at RT, but with a refined mesh.

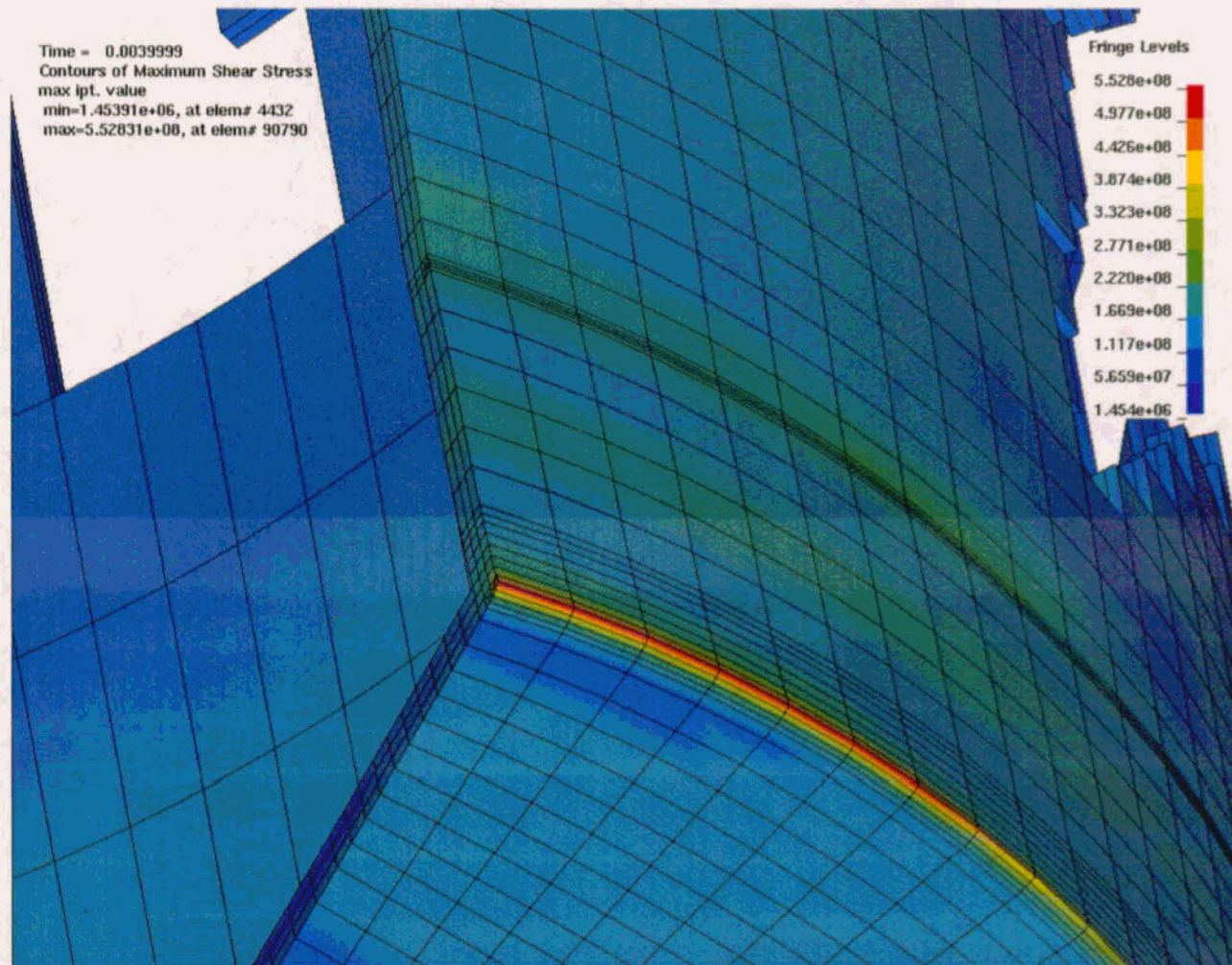


Figure 6-3. Outer Shell Refined Mesh at Room Temperature (Pa)

Figure 6-3 shows that the maximum stress intensity in the OS at RT is 1110 MPa at 0.004 seconds, with the refined mesh. Figure 6-4 may be found on the next page. It shows the maximum shear stress in the inner shell at RT, but with a refined mesh.

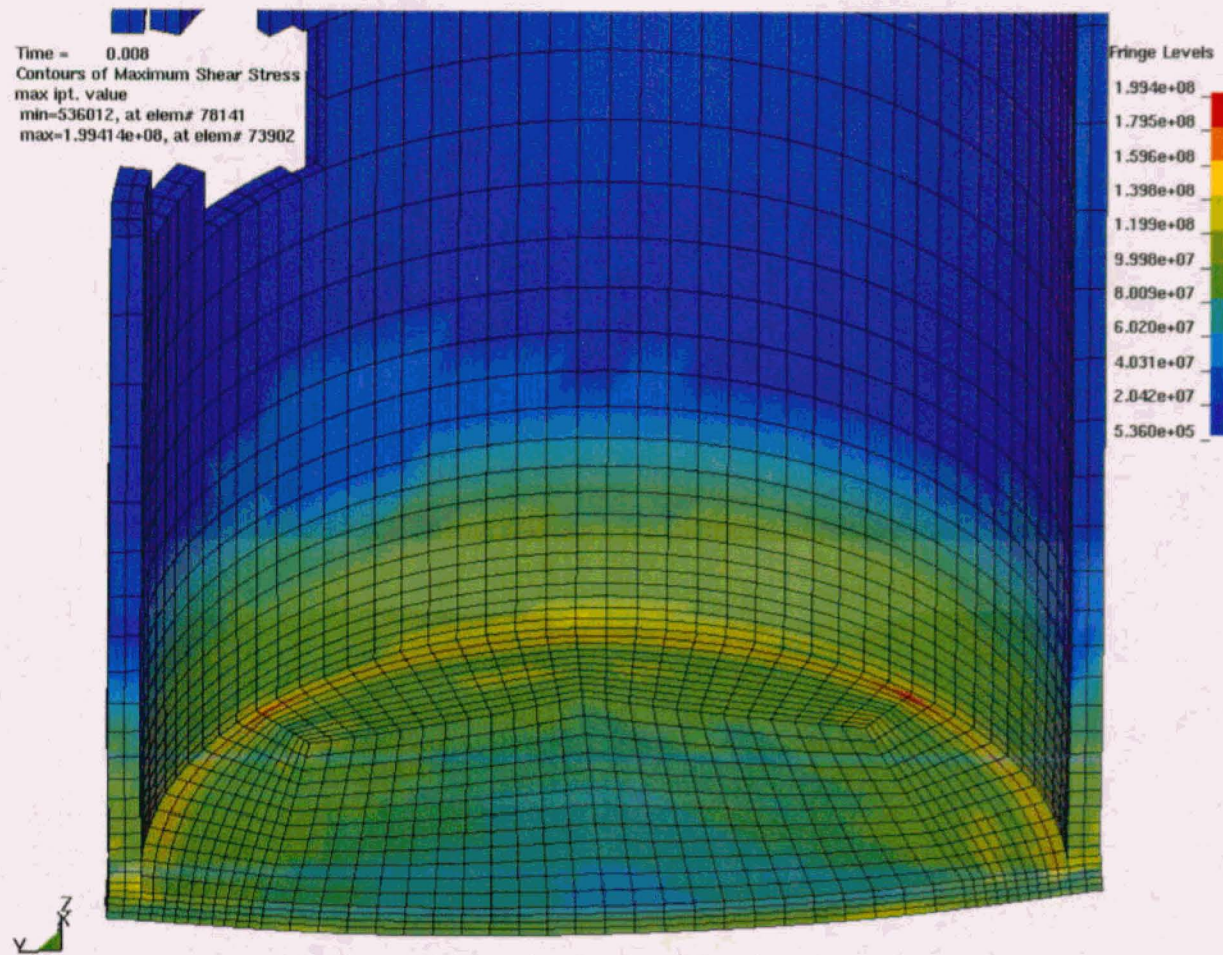


Figure 6-4. Inner Shell Refined Mesh at Room Temperature (Pa)

Figure 6-4 figure shows that the maximum stress intensity in the IS at RT is 399 MPa at 0.008 seconds. Table 6-1 shows a comparison of the results from the refined mesh with the standard mesh.

Table 6-1. Mesh Verification

Standard Mesh		Refined Mesh		% Change
OS	El# 76236	$V = 1.5963e-6 \text{ m}^3$ $\tau_{\max} = 5.1648e+8 \text{ Pa}$	El# 90790	$V = 8.4923e-7 \text{ m}^3$ $\tau_{\max} = 5.52831e+8 \text{ Pa}$
	El# 60866	$V = 9.5294e-6 \text{ m}^3$ $\tau_{\max} = 1.99063e+8 \text{ Pa}$	El# 73902	$V = 7.1471e-6 \text{ m}^3$ $\tau_{\max} = 1.99414e+8 \text{ Pa}$

For both the OS and the IS, the percent changes in stress are approximately one order of magnitude less than the percent changes in volume of the element. Thus, the standard mesh is deemed acceptable, and this mesh will be used throughout the rest of this calculation.

Figure 6-5 may be found on the next page. It shows the maximum shear stress in the OS at 400 °F.

Originator: AKS Date: OCT 09, 2002 Checker: VB Date: 10/04/02

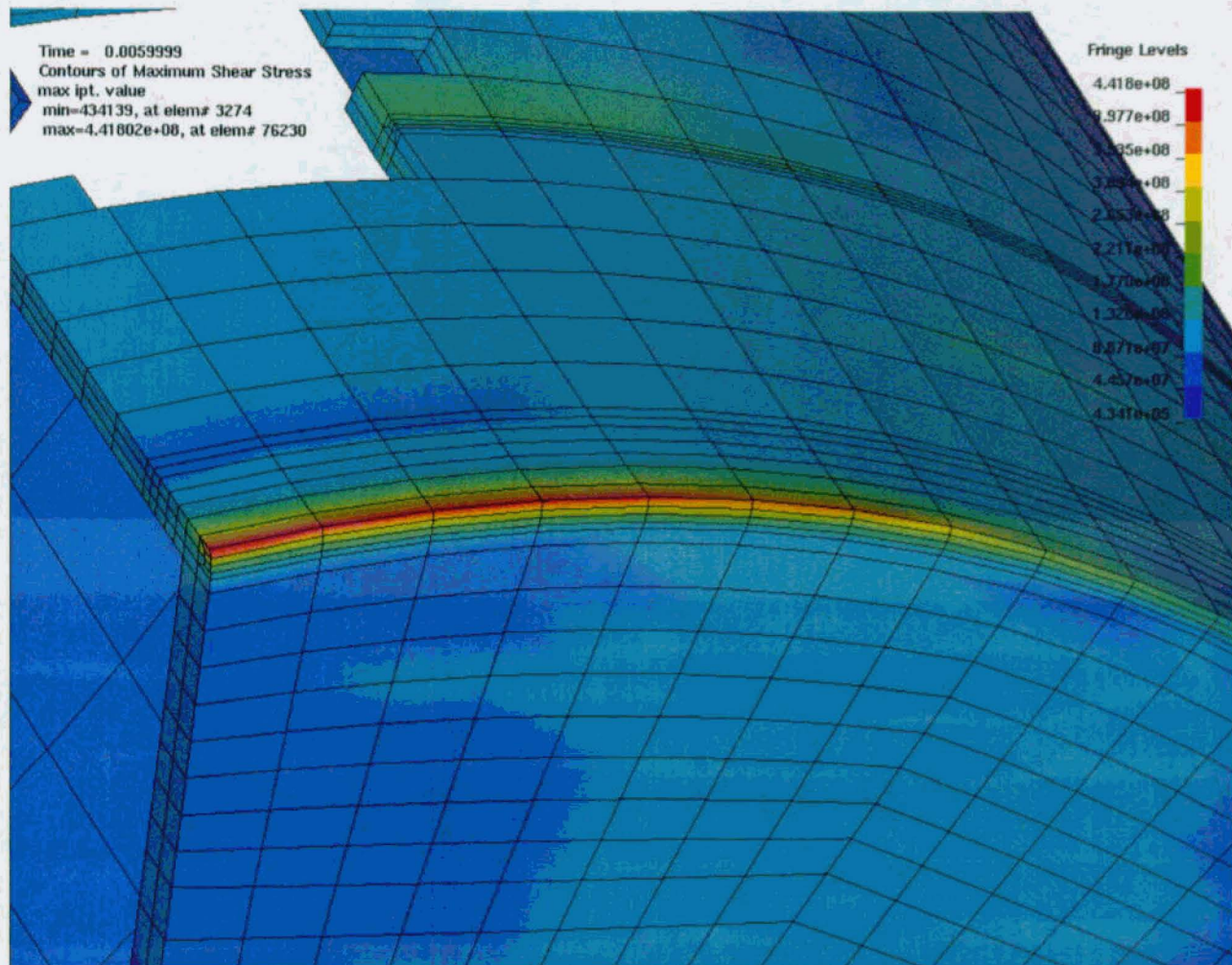


Figure 6-5. Outer Shell at 400 °F (Pa)

Figure 6-5 shows that the maximum stress intensity in the OS is 884 MPa at 0.006 seconds. Figure 6-6 may be found on the next page. It shows the maximum shear stress in the IS at 400 °F.

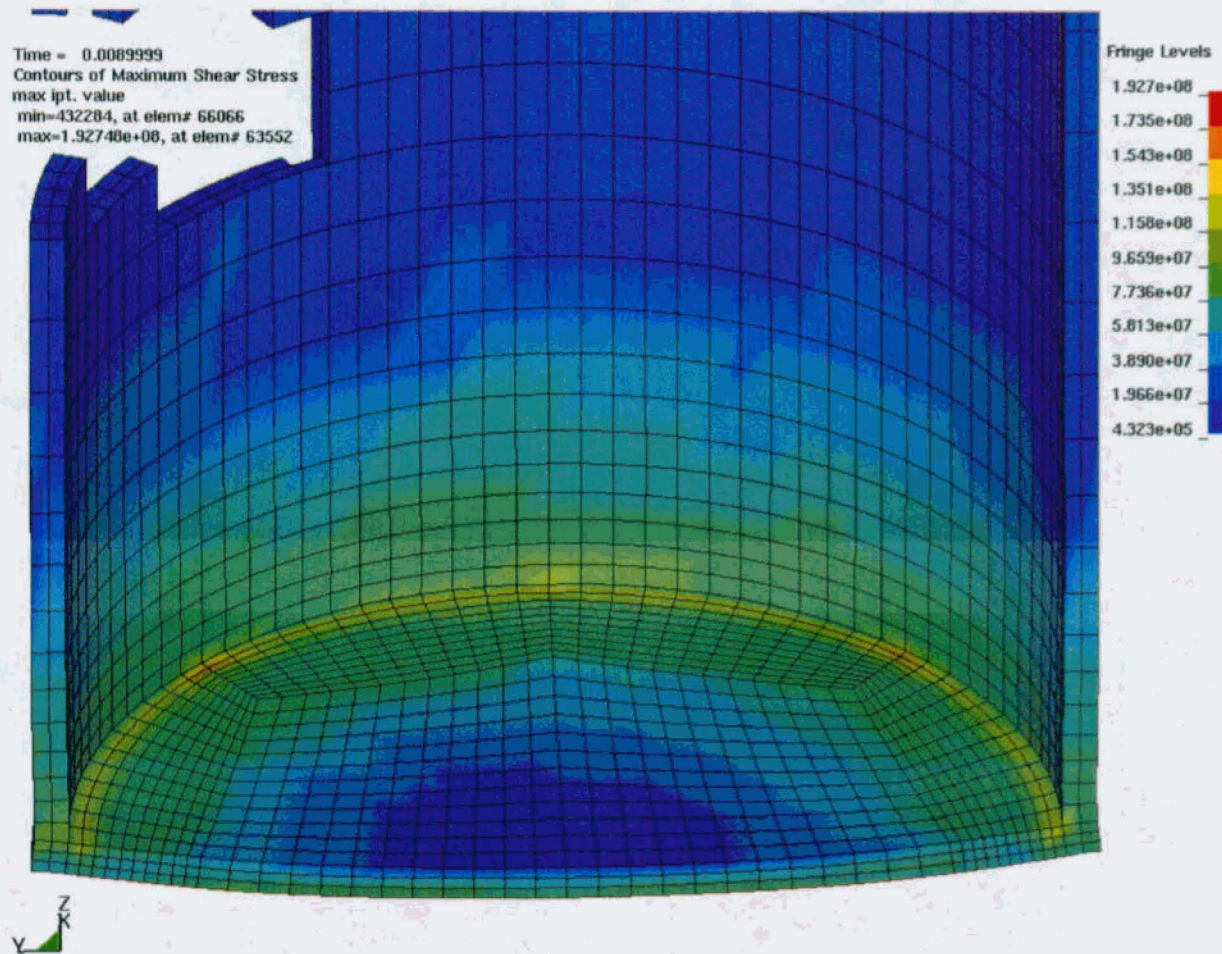


Figure 6-6. Inner Shell at 400 °F (Pa)

Figure 6-6 shows that the maximum stress intensity in the IS is 385 MPa at 0.009 seconds. Figure 6-7 may be found on the next page. It shows the maximum shear stress in the OS at 600 °F.

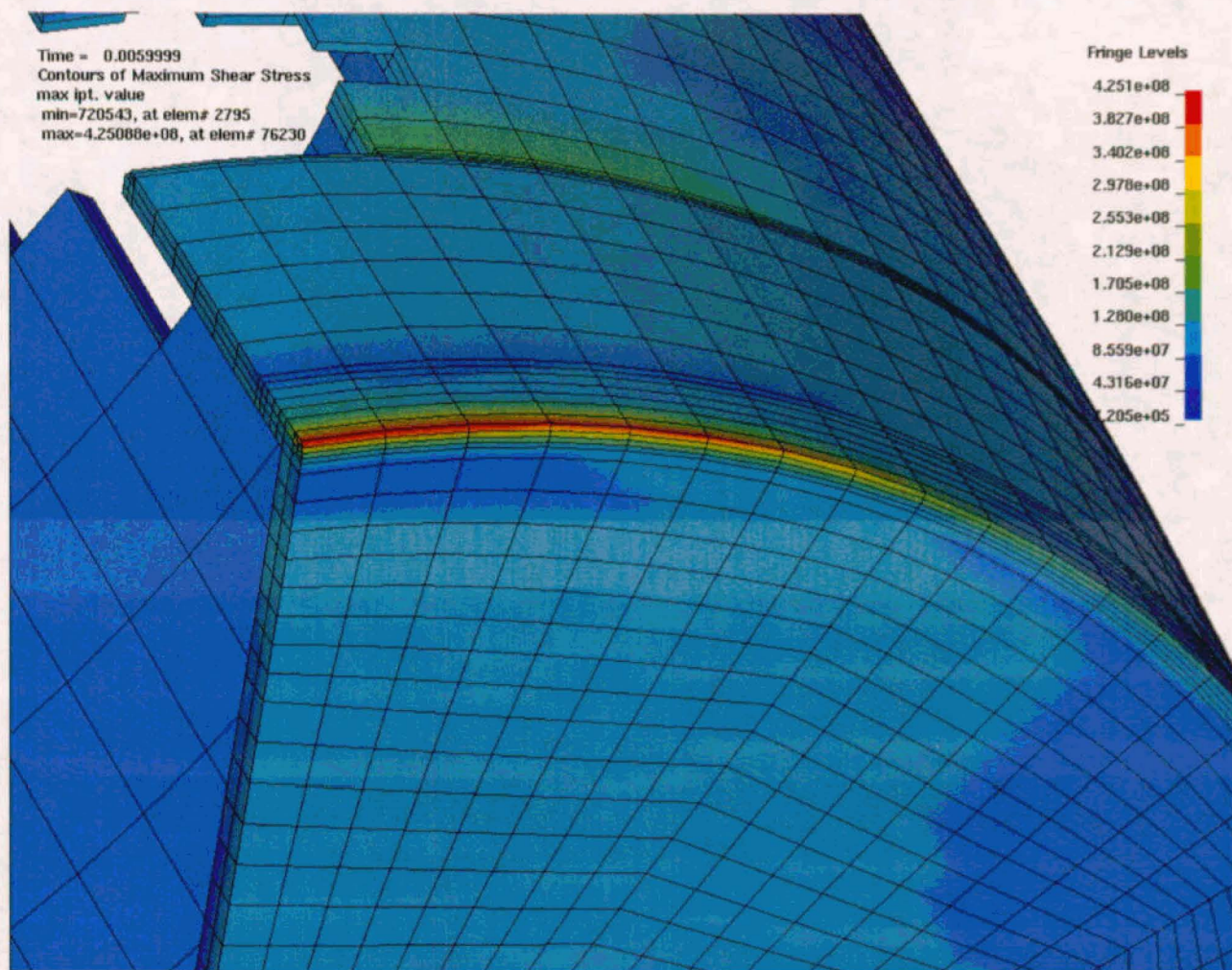


Figure 6-7. Outer Shell at 600 °F (Pa)

Figure 6-7 shows that the maximum stress intensity in the OS is 850 MPa at 0.006 seconds. Figure 6-8 may be found on the next page. It shows the maximum shear stress in the IS at 600 °F.

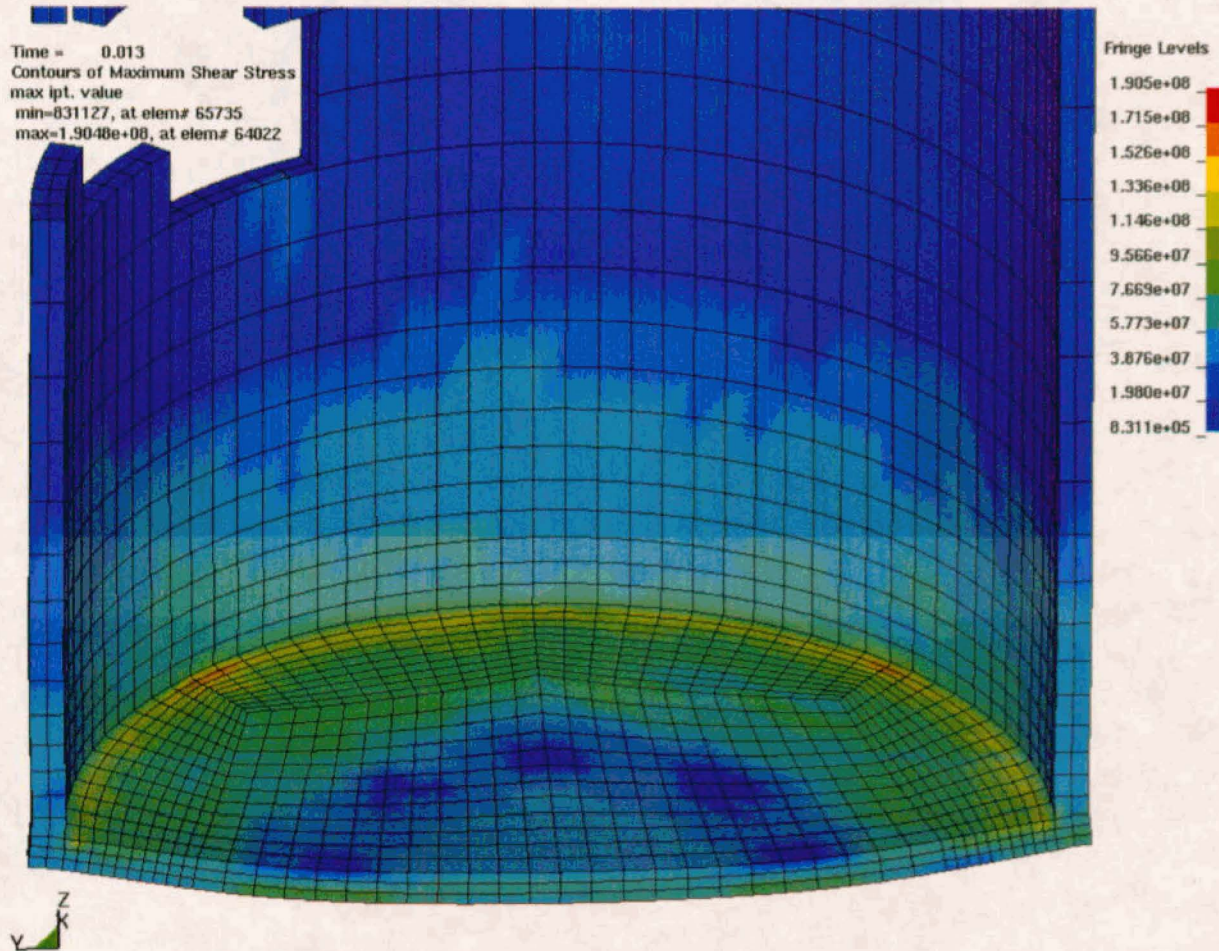


Figure 6-8. Inner Shell at 600 °F (Pa)

Figure 6-8 shows that the maximum stress intensity in the IS is 381 MPa at 0.013 seconds. Figure 6-9 may be found on the next page. It shows the maximum shear stress in the OS at 600 °F, but using elongation at elevated temperatures based on vendor data.

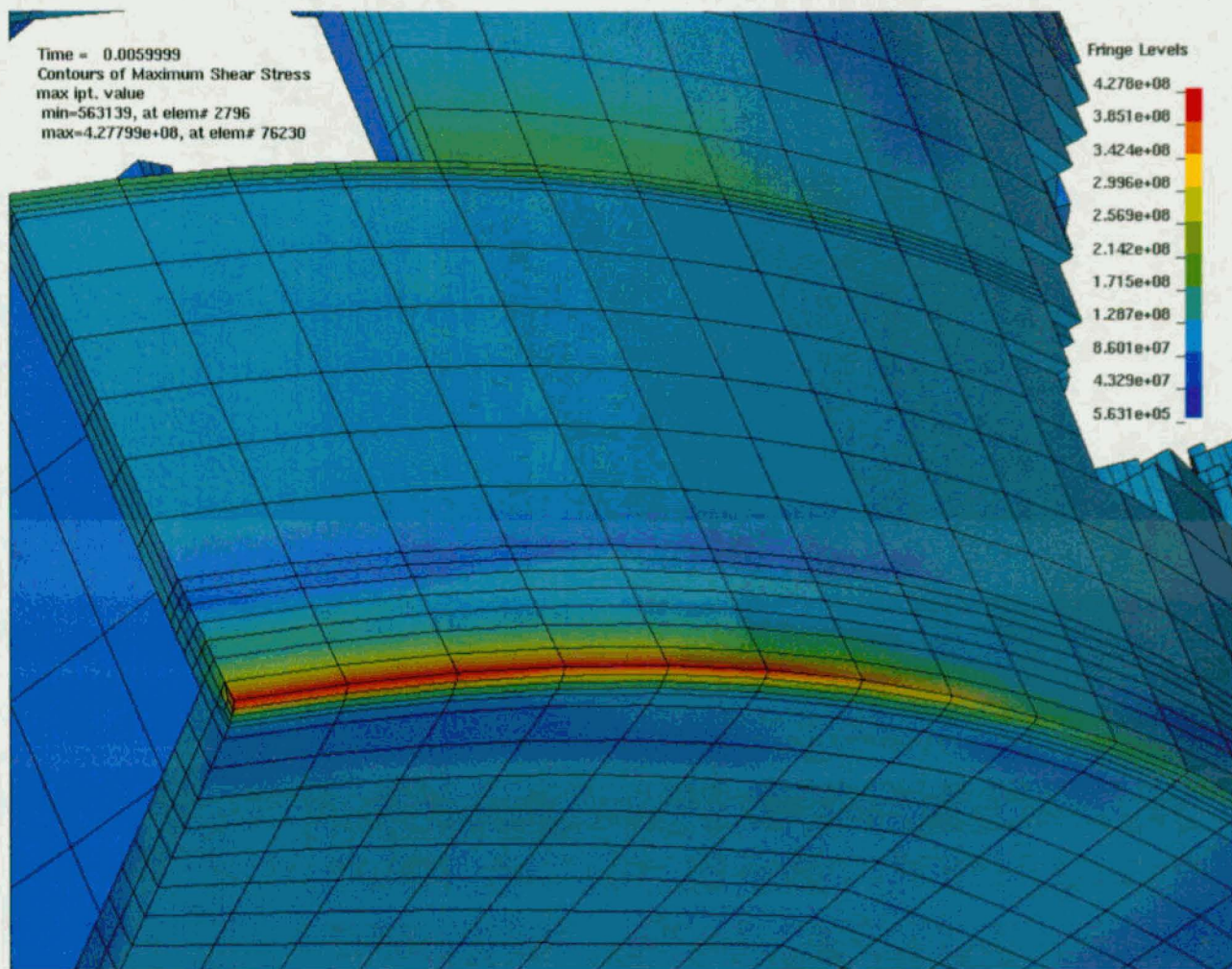


Figure 6-9. Outer Shell at 600 °F with Vendor Elongation (Pa)

Figure 6-9 shows that the maximum stress intensity in the OS is 856 MPa at 0.006 seconds. Figure 6-10 may be found on the next page. It shows the maximum shear stress in the IS at 600 °F, but using elongation at elevated temperatures based on vendor data.

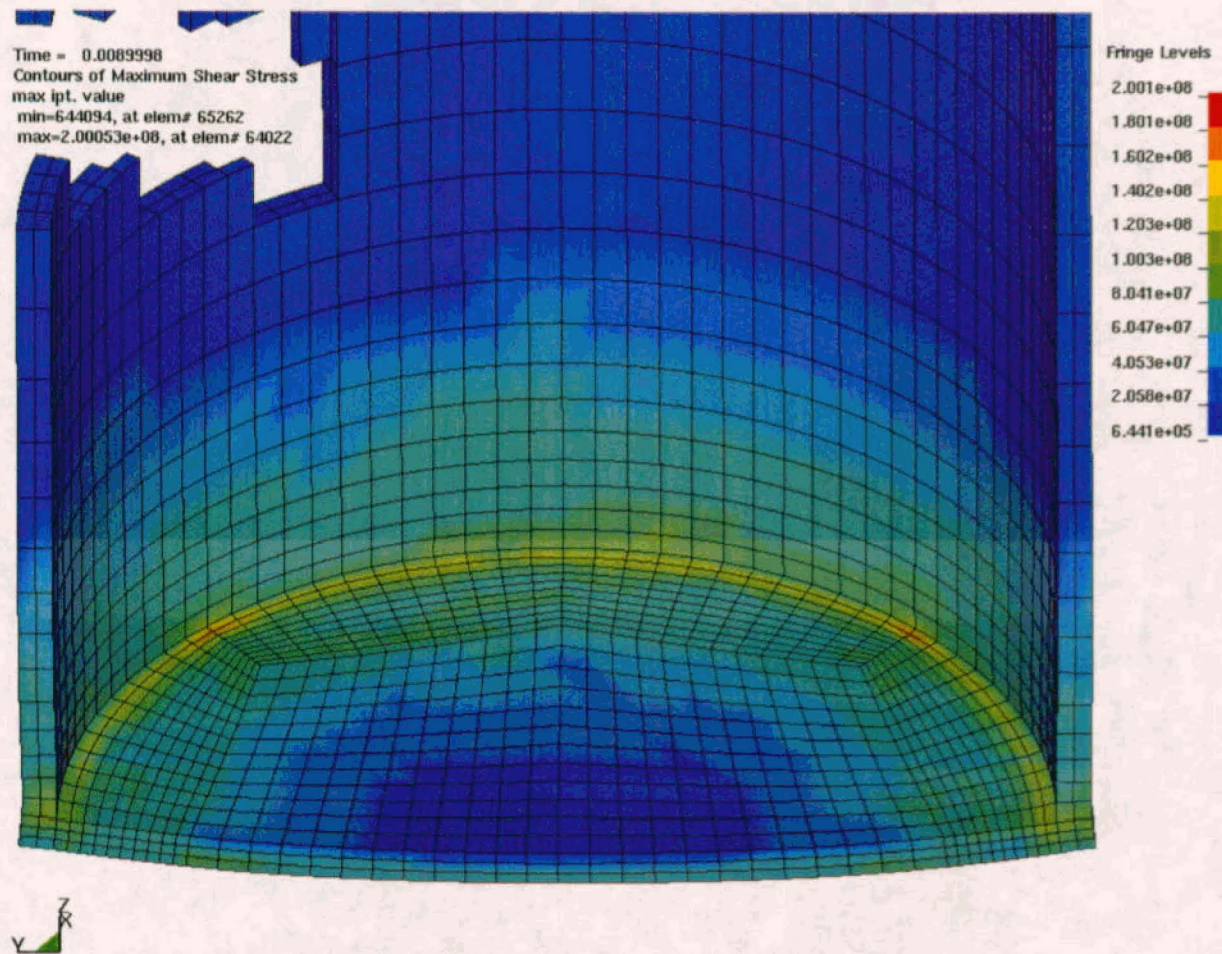


Figure 6-10. Inner Shell at 600 °F with Vendor Elongation (Pa)

Figure 6-10 shows that the maximum stress intensity in the inner shell is 400 MPa at 0.009 seconds.

Table 2 shows a comparison of observed stress to allowable stress.

Table 6-2. Maximum Stress by Load Case.

Part	Temperature	Elongation Value	Max Stress Intensity	$\sigma_{int} / \sigma_{allowable}$
IS	70 °F	ASME	398 MPa	0.629
OS	70 °F	ASME	1030 MPa	1.18
IS	400 °F	ASME	385 MPa	0.633
OS	400 °F	ASME	884 MPa	1.06
IS	600 °F	ASME	381 MPa	0.629
OS	600 °F	ASME	850 MPa	1.07
IS	600 °F	ASME - 30%	400 MPa	0.718
OS	600 °F	ASME + 10%	856 MPa	1.04

Note: $\sigma_{allowable}$ is equal to 90% of σ_u .

As was stated earlier, the regions in the OS where the stress intensity is maximum does not extend through the thickness of the OS. Therefore, the regions where $\sigma_{int}/\sigma_{allowable}$ exceeds a value of 1 do not extend through the OS wall. This may be verified by examining the figures that contain the OS.

The output values are reasonable for the given inputs in this calculation. The uncertainties are taken into account by consistently using the most conservative approach; the calculations, therefore, yield a conservatively bounding set of results. The results are suitable for assessing the stress state of the IS and OS during a vertical drop event.

7. REFERENCES

1. BSC (Bechtel SAIC Company) 2001. *Uncanistered Spent Nuclear Fuel Disposal Container System Description Document*. SDD-UDC-SE-000001 REV 01 ICN 01. Las Vegas, Nevada: Bechtel SAIC Company. ACC: MOL.20010927.0070.
2. ASME (American Society of Mechanical Engineers) 2001. *2001 ASME Boiler and Pressure Vessel Code*. New York, New York: American Society of Mechanical Engineers. TIC: 251425.
3. ASM International 1990. *Properties and Selection: Irons, Steels, and High-Performance Alloys*. Volume 1 of *Metals Handbook*. 10th Edition. Materials Park, Ohio: ASM International. TIC: 245666.
4. CRWMS M&O 1999. *Classification of the MGR Uncanistered Spent Nuclear Fuel Disposal Container System*. ANL-UDC-SE-000001 REV 00. Las Vegas, Nevada: CRWMS M&O. ACC: MOL.19990928.0216.
5. ASM (American Society for Metals) 1961. *Properties and Selection of Metals*. Volume 1 of *Metals Handbook*. 8th Edition. Pages 506-507. Metals Park, Ohio: American Society for Metals. TIC: 252319.
6. Haynes International 1997. *Hastelloy C-22 Alloy*. Kokomo, Indiana: Haynes International. TIC: 238121.
7. CRWMS M&O 2000. *Software Code: LS-DYNA*. V950. HP 9000. 10300-950-00.
8. Boyer, H.E., ed. 2000. *Atlas of Stress-Strain Curves*. Metals Park, Ohio: ASM International. TIC: 248901.
9. AP-SI.1Q, Rev. 3, ICN 4. *Software Management*. Washington, D.C.: U.S. Department of Energy, Office of Civilian Radioactive Waste Management. ACC: MOL.20020520.0283.
10. Dieter, G.E. 1976. *Mechanical Metallurgy*. 2nd Edition. Materials Science and Engineering Series. New York, New York: McGraw-Hill Book Company. TIC: 247879.
11. AP-3.12Q, Rev. 1, ICN 2. *Design Calculations and Analyses*. Washington, D.C.: U.S. Department of Energy, Office of Civilian Radioactive Waste Management. ACC: MOL.20020607.0013.
12. CRWMS M&O 2000. *Stress-Strain-Curve Character for Alloy C-22 and 316 Stainless Steel*. Input Transmittal 00384.T. Las Vegas, Nevada: CRWMS M&O. ACC: MOL.20001013.0053.

13. ASM (American Society for Metals) 1980. *Properties and Selection: Stainless Steels, Tool Materials and Special-Purpose Metals*. Volume 3 of *Metals Handbook*. 9th Edition. Benjamin, D., ed. Metals Park, Ohio: American Society for Metals. TIC: 209801.
14. ASTM G 1-90 (Reapproved 1999). 1999. *Standard Practice for Preparing, Cleaning, and Evaluating Corrosion Test Specimens*. West Conshohocken, Pennsylvania: American Society for Testing and Materials. TIC: 238771.
15. CRWMS M&O 1997. *Waste Container Cavity Size Determination*. BBAA00000-01717-0200-00026 REV 00. Las Vegas, Nevada: CRWMS M&O. ACC: MOL.19980106.0061.
16. DOE (U.S. Department of Energy) 2002. *Quality Assurance Requirements and Description*. DOE/RW-0333P, Rev. 12. Washington, D.C.: U.S. Department of Energy, Office of Civilian Radioactive Waste Management. ACC: MOL.20020819.0387.
17. High Temp Metals. 2002. "17-4Ph Technical Data." Sylmar, California: High Temp Metals. Accessed March 19, 2002. TIC: 252170. <http://www.hightempmetals.com/hitemp17-4PHdata.htm>
18. Allegheny Ludlum. 1987. Technical Data Blue Sheet for Stainless Steels Chromium-Nickel-Molybdenum, Types 316, 316L, 317, and 317L. Pittsburgh, Pennsylvania: Allegheny Ludlum Corporation. TIC: 240370.
19. AP-3.13Q, Rev. 3, ICN 1. *Design Control*. Washington, D.C.: U.S. Department of Energy, Office of Civilian Radioactive Waste Management. ACC: MOL.20020925.0444.
20. McKenzie, D.G., IV. 2002. *Waste Package Design Methodology Report*. TDR-MGR-MD-000006 REV 02. Las Vegas, Nevada: Bechtel SAIC Company. ACC: MOL.20020404.0085.

8. ATTACHMENTS

Attachment I (on compact disc): contains electronic files (see Table 8-1 for a complete list). The *.k files are input files for LS-DYNA. The d3hsp files are LS-DYNA output files. *.tg files are TrueGrid input files.

Attachment II (4 pages): Design sketch (*44-BWR Waste Package Concept for License Application* [SK-0220 REV 01, 4 sheets])

Attachment III (5 pages): Design sketch (*Waste Package Lifting Collars* [SK-0234 REV 01, 5 sheets])

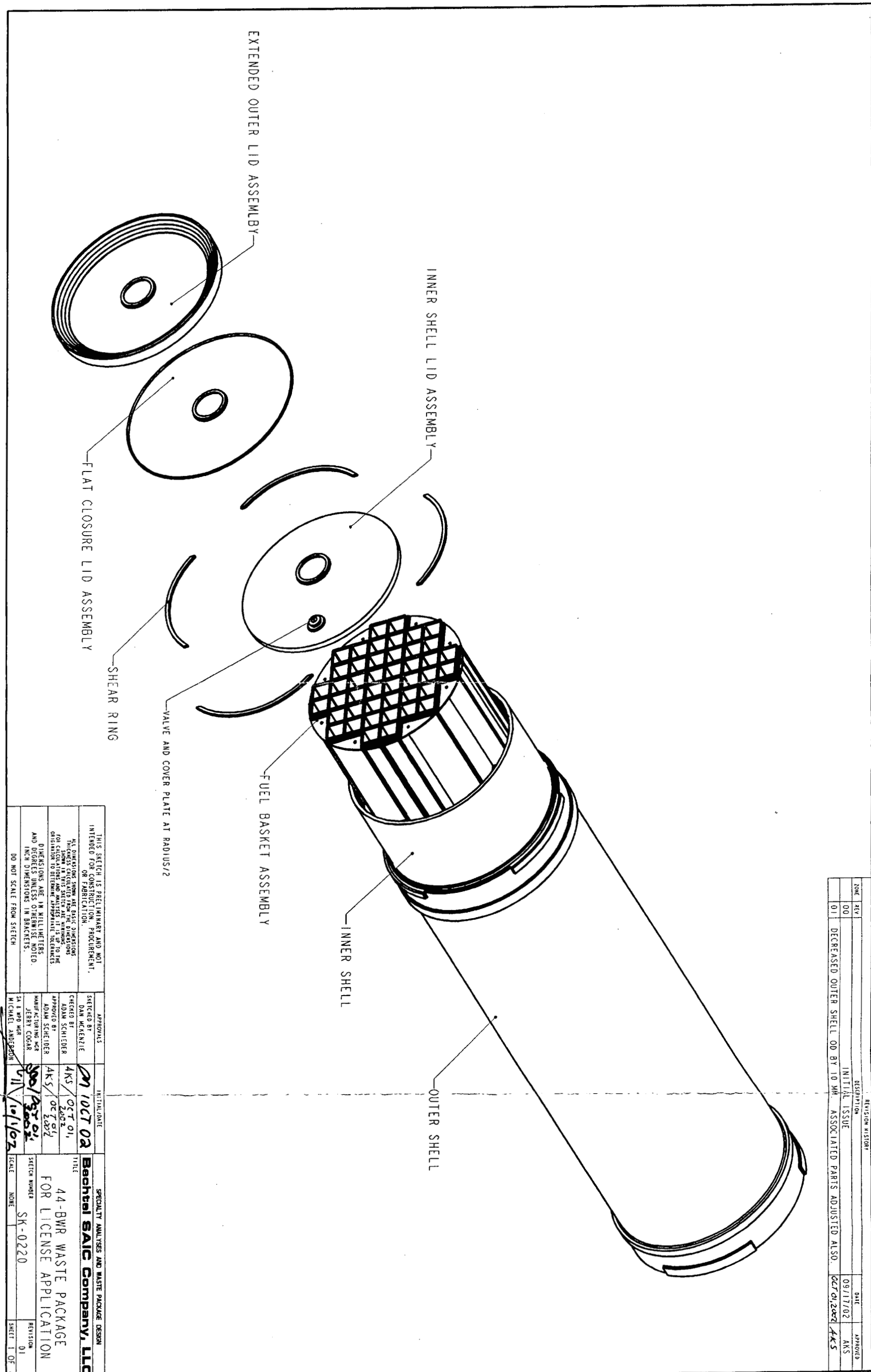
Table 8-1 provides a list of files submitted in the form of electronic files (compact disc) in Attachment I.

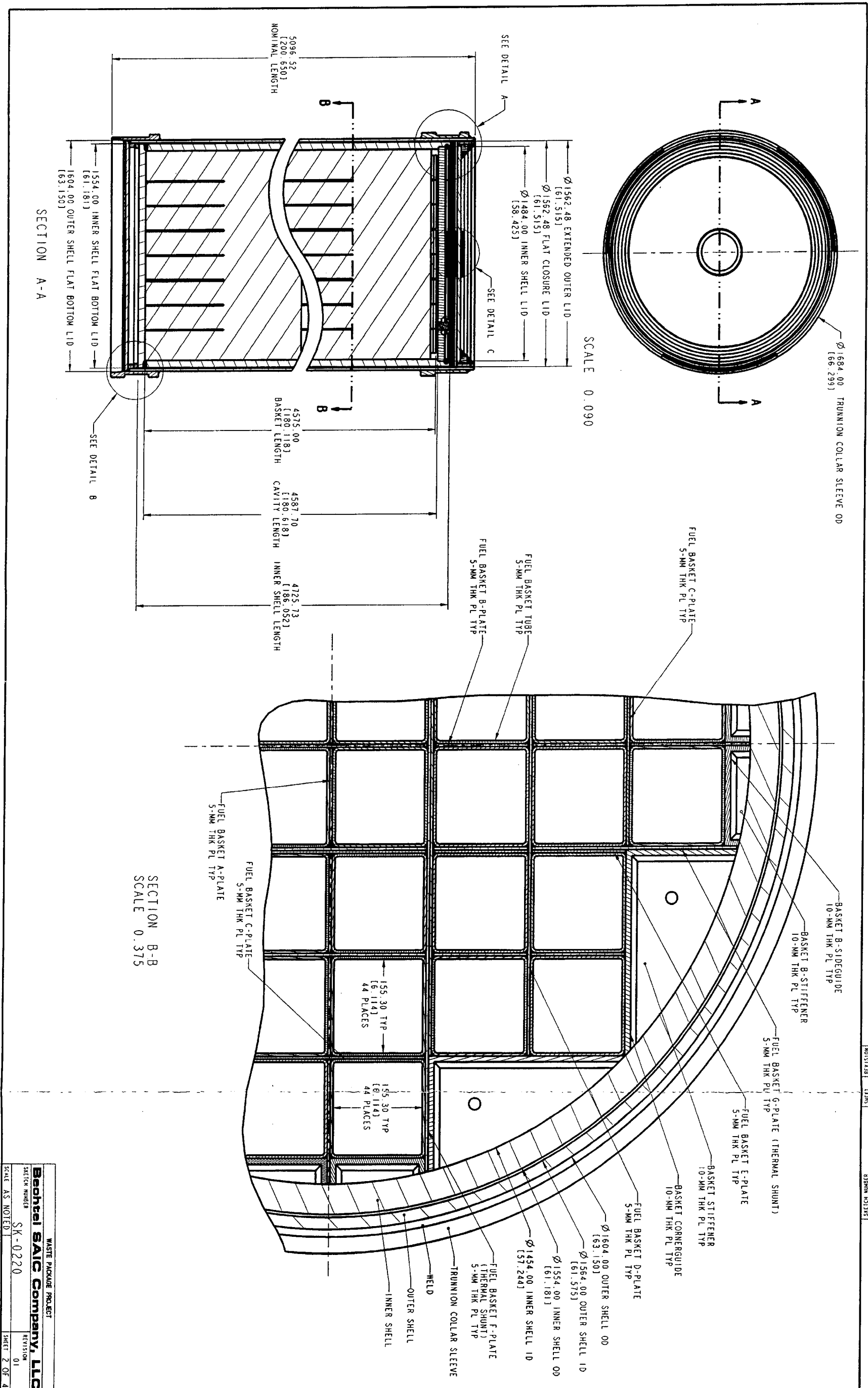
Table 8-1. List of Files Submitted in the Form of Electronic Files in Attachment I

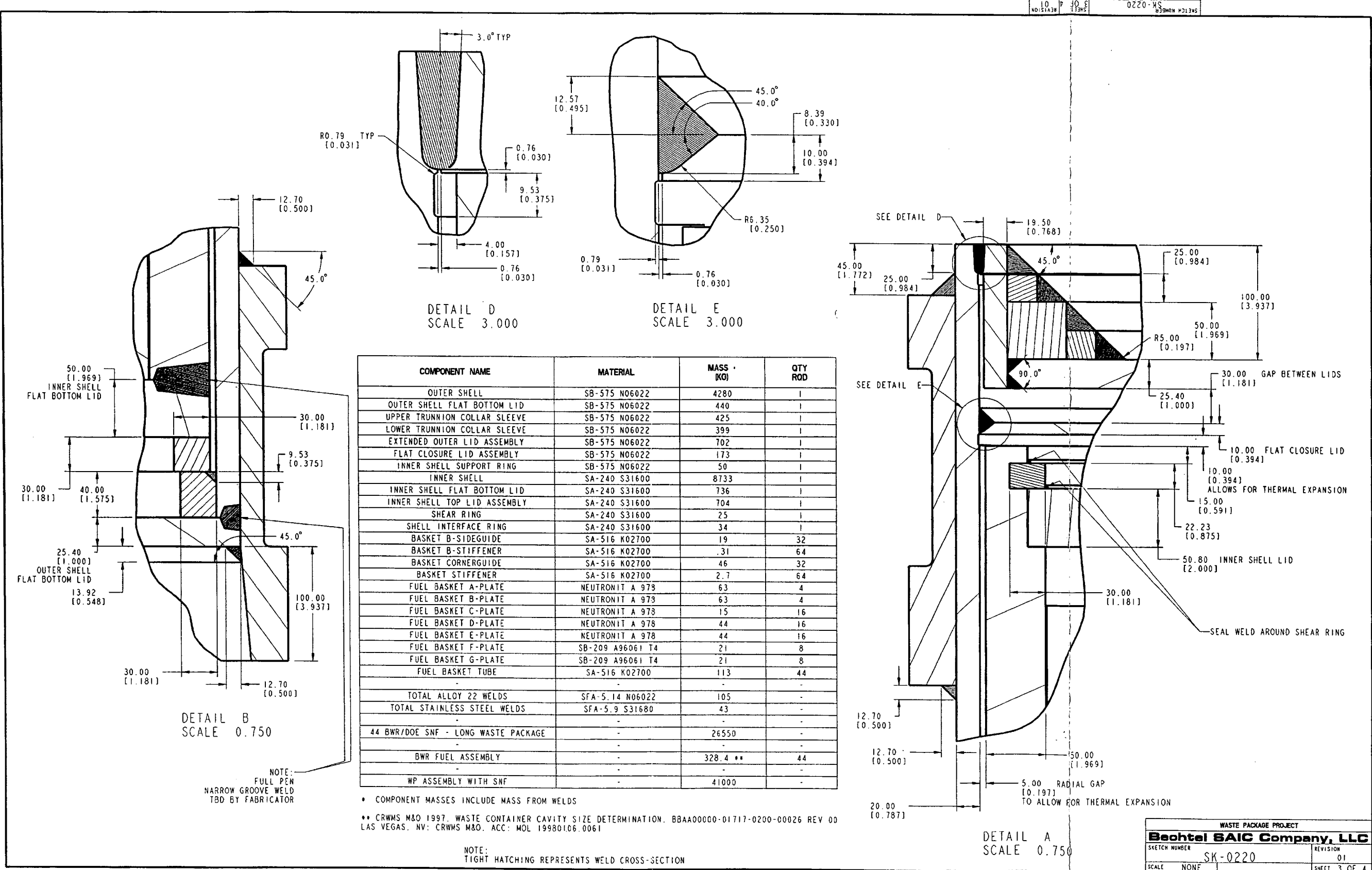
Description	Date	Time	Size
b44.tg	SEP 27, 2002	11:05 am	25 KB
b44ref.tg	SEP 17, 2002	9:20 am	24 KB
Subfolder "400"			
d3hsp	SEP 27, 2002	11:06 am	28,201 KB
b446.k	SEP 27, 2002	11:06 am	10,257 KB
Subfolder "600"			
d3hsp	SEP 27, 2002	11:06 am	28,201 KB
b446v.k	SEP 27, 2002	11:06 am	10,257 KB
Subfolder "600v"			
d3hsp	SEP 27, 2002	11:07 am	28,193 KB
b446v.k	SEP 27, 2002	11:07 am	10,257 KB
Subfolder "RT"			
d3hsp	SEP 27, 2002	11:06 am	28,216 KB
b44RT.k	SEP 27, 2002	11:06 am	10,257 KB
Subfolder "RT_refined"			
d3hsp	SEP 17, 2002	9:26 am	32,723 KB
b44ref.k	SEP 17, 2002	9:26 am	12,057 KB

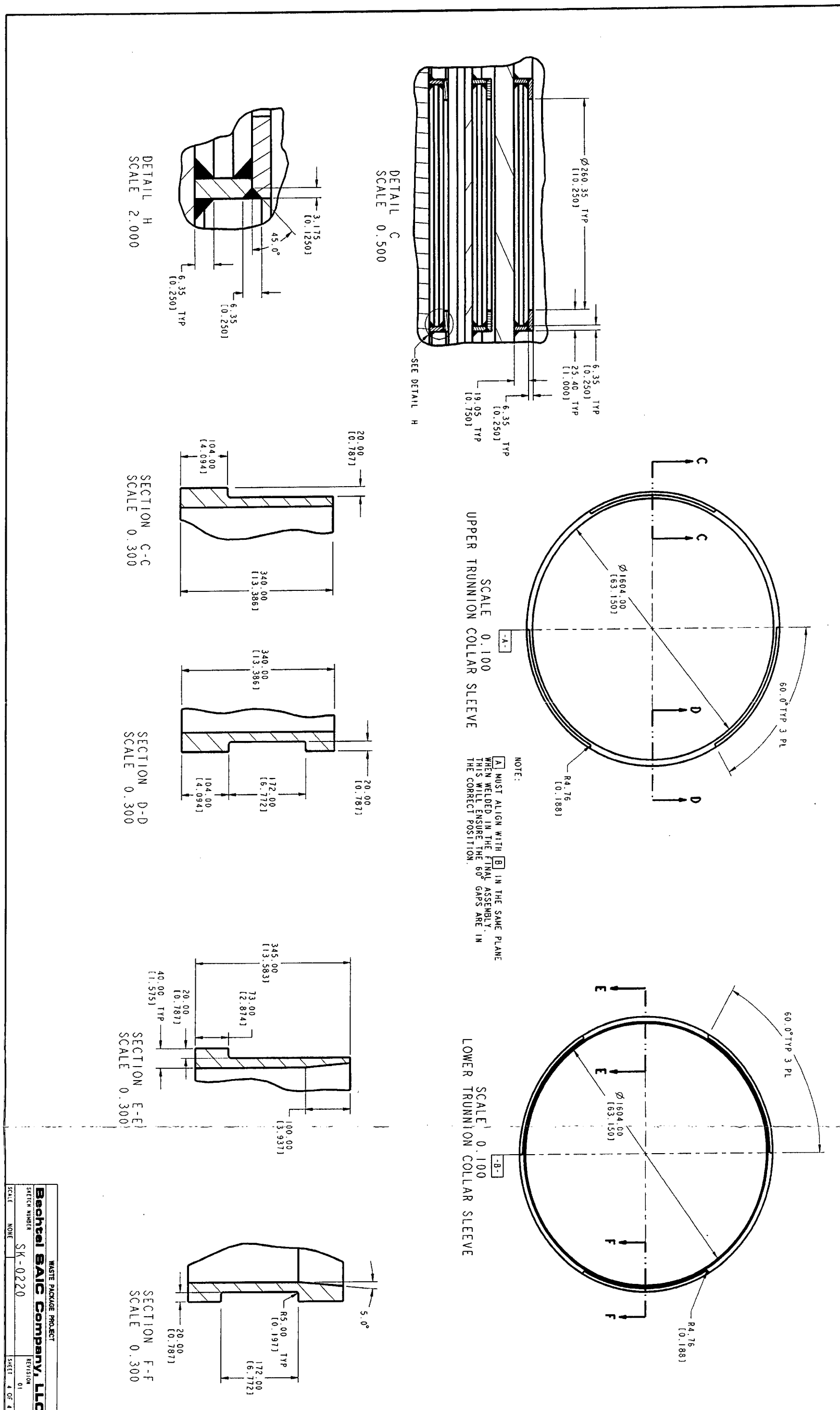
NOTE: The file sizes may vary with operating system.

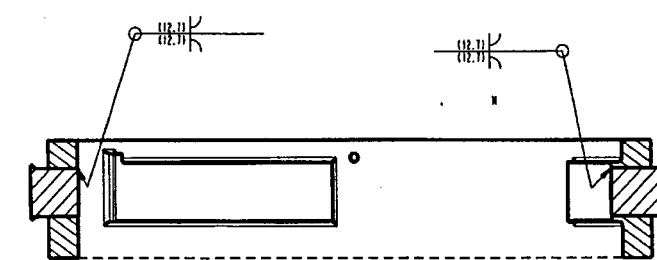
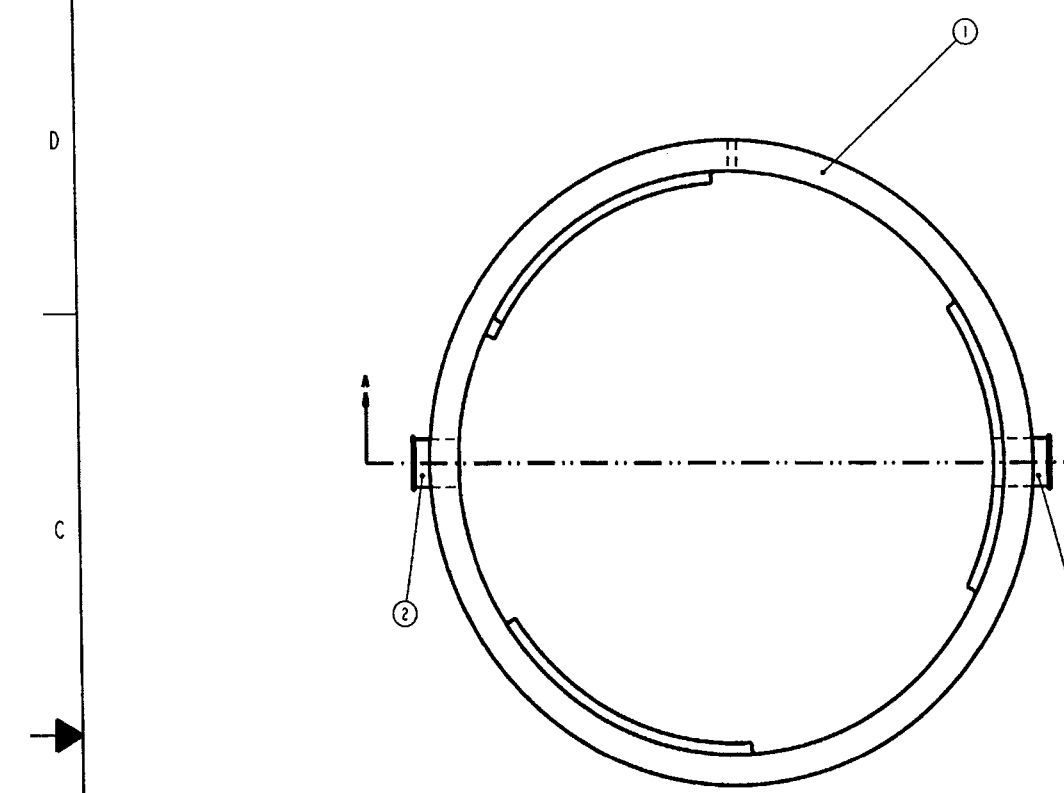
Title: Vertical Drop of 44-BWR Waste Package with Lifting Collars
 Document Identifier: 000-00C-DSU0-00800-000-00A











SECTION A-A

ALL SHEETS ARE THE SAME REVISION STATUS

ZONE	REV	DESCRIPTION	DATE	APPROVED
-	00	INITIAL ISSUANCE	FEB 15, 2002	AKS
MANY	01	USE ONE STOP ON LIFTING FEATURES INSTEAD OF THREE		
A1-D1	01	CHANGE TITLE FROM "21-PWR LIFTING COLLARS" TO "WASTE PACKAGE LIFTING COLLARS"		
MANY	01	MODIFY SHAPE AND PLACEMENT OF TRUNNIONS		
-	01	CONDENSED TRUNNIONS TO ONE PAGE, REMOVED PAGE 06 FROM REV 00		
-	01	ADD MASSES AND DIMENSIONS FOR DIFFERENT WASTE PACKAGES		

PART NO.	PART	MATERIAL	QUANTITY
1	UPPER LIFTING COLLAR	SA-705 FORGING	1
2	SHORT TRUNNION	SA-564 BAR	1
3	LONG TRUNNION	SA-564 BAR	1

WASTE PACKAGE	ASSEMBLY MASS (KG)
NAVAL	1.69e3
12-PWR	1.18e3
5-DHLW	1.82e3
44-BWR	1.46e3
21-PWR	1.44e3

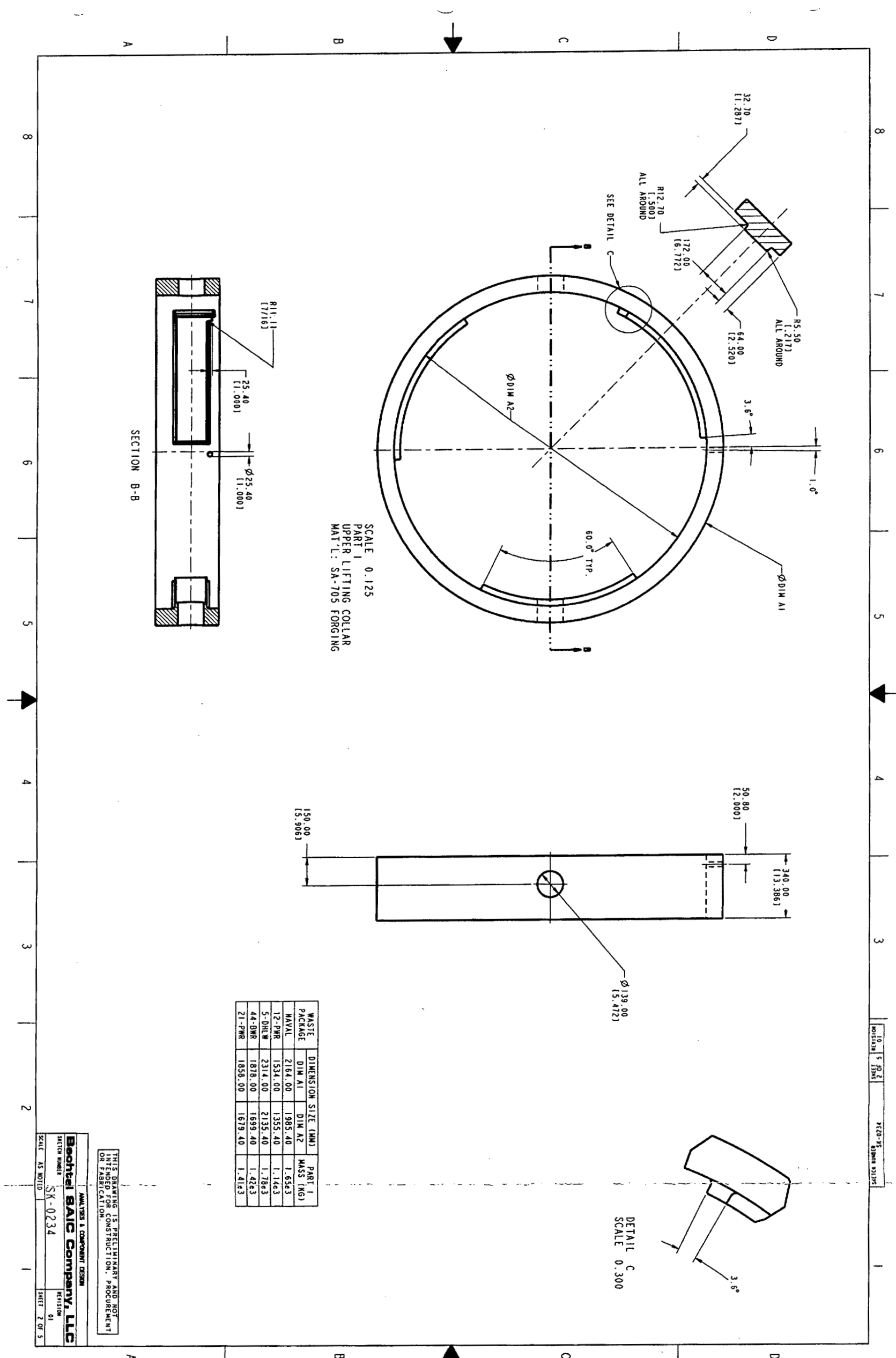
NOTE 1: WELD SHOULD BE MACHINED FLUSH WITH SURFACE WHERE APPLICABLE. ON SIDE WITH SHOULDER, THE TRUNNION SHOULD BE INSERTED, WELDED, THEN MACHINED TO THE FINAL DIMENSIONS AFTER HEAT TREATING. THE TRUNNION AND COLLAR SHOULD BE SEAMLESS WHEN VIEWED FROM THE INSIDE. AWS E630 WELD WIRE TO BE USED.

NOTE 2: SURFACES SHOULD BE MACHINED FLUSH WITH MATING SURFACES WHERE APPLICABLE AFTER HEAT TREATING. AWS E630 WELD WIRE TO BE USED.

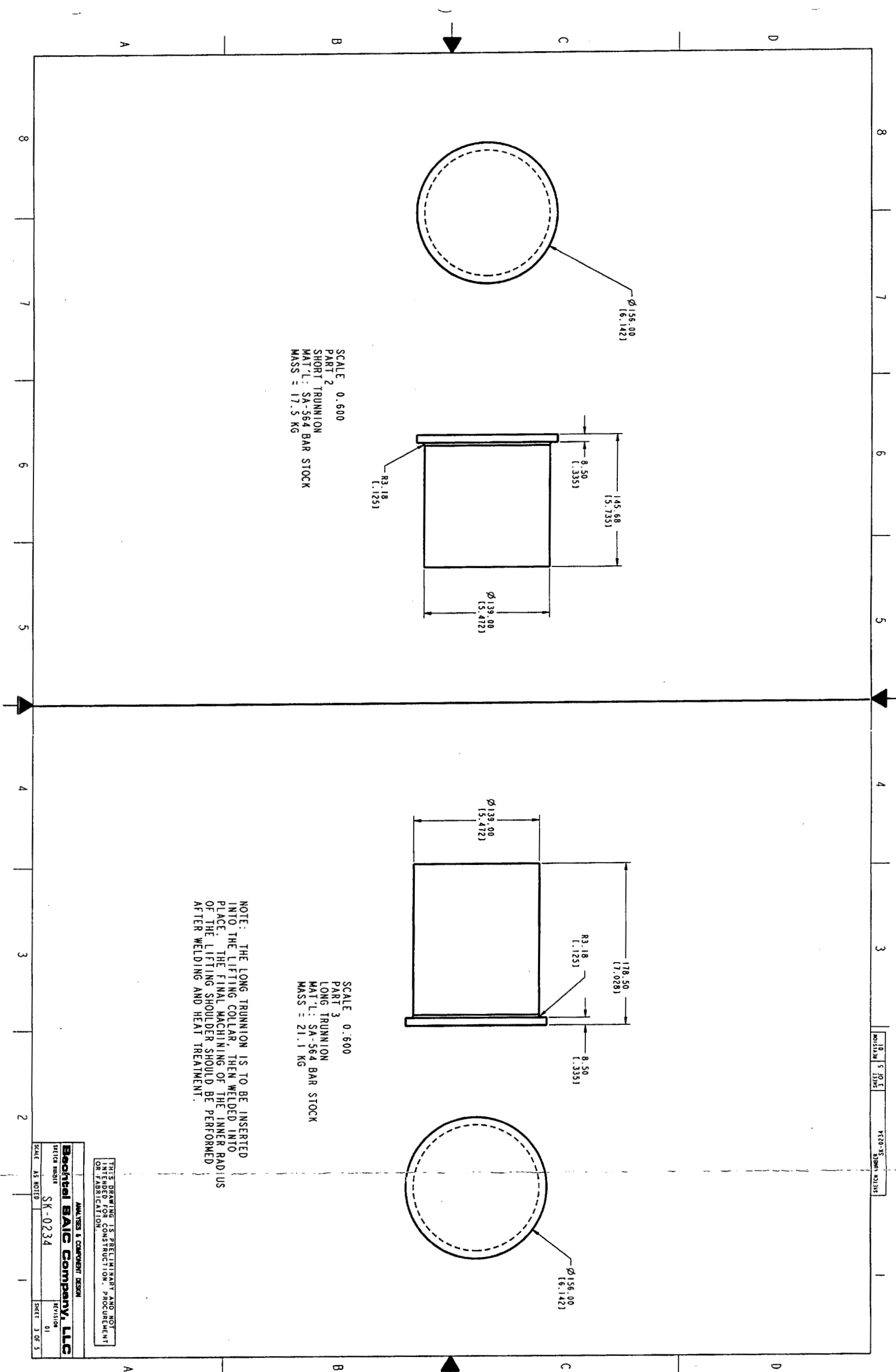
NOTE 3: ENTIRE ASSEMBLY SHOULD BE HEAT TREATED TO CONDITION H900 (HEAT SOLUTION-TREATED MATERIAL AT 900°F FOR 1 HOUR AND AIR COOL). ALL EDGES SHOULD BE BURR-FREE.

THIS DRAWING IS PRELIMINARY AND NOT INTENDED FOR CONSTRUCTION, PROCUREMENT, OR FABRICATION.		
"FOR INFORMATION ONLY"	APPROVALS	INITIAL DATE
THIRD ANGLE PROJECTION	SKETCHED BY ADAM SCHEIDER	4/25/2002
	CHECHED BY TIN SCHMITT	TS 4/24/02
	APPROVED BY ADAM SCHEIDER	4/25/2002
DIMENSIONS ARE IN MILLIMETERS AND DEGREES UNLESS OTHERWISE NOTED	MANUFACTURING MGR JERRY COGAR	4/25/2002
DO NOT SCALE FROM SKETCH	DESIGN GROUP MGR MICHAEL ANDERSON	4/25/2002
		SK-0234
		REVISION 01
		SCENE, AS NOTED
		SHEET 1 OF 5

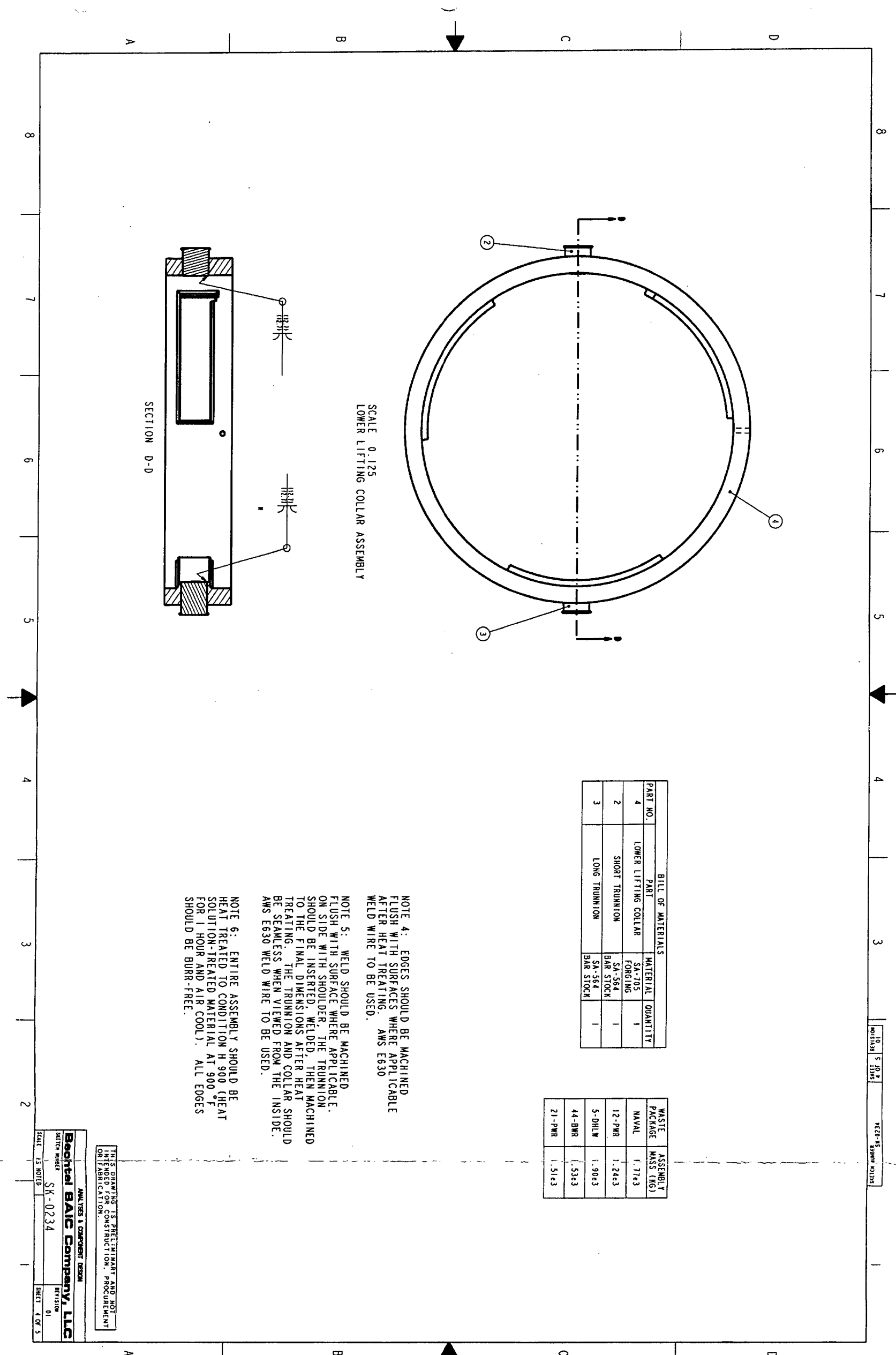
Title: Vertical Drop of 44-BWR Waste Package with Lifting Collars
Document Identifier: 000-00C-DSU0-00800-000-00A



Title: Vertical Drop of 44-BWR Waste Package with Lifting Collars
 Document Identifier: 000-00C-DSU0-00800-000-00A



Title: Vertical Drop of 44-BWR Waste Package with Lifting Collars
 Document Identifier: 000-00C-DSU0-00800-000-00A



Title: Vertical Drop of 44-BWR Waste Package with Lifting Collars

Document Identifier: 000-00C-DSU0-00800-000-00A

—
A
B

D —

8 7 6 5 4 3

10 9 8 7 6 5 4 3

ME-0234

SECTION F-F

SEE DETAIL E

1.0°

3.6°

Ø DIM A3

60.0° TYP

Ø DIM A4

112.70 [4.4371]

R5.50 [.2171] ALL AROUND

172.00 [6.7721]

R12.70 [.5001] ALL AROUND

32.70 [1.287]

SCALE 0.125
PART 4
LOWER LIFTING COLLAR
MAT'L: SA-705 FORGING

198.70 [7.823]

50.80 [2.000]

357.70 [14.083]

Ø 139.00 [5.472]

3.6°

DETAIL E
SCALE 0.300

R11.11 [7/16]

25.40 [1.000]

Ø 25.40 [1.000]

WASTE PACKAGE DIMENSION SIZE (MM) PART 4 MASS (KG)

NAVAL 2164.00 1985.40 1.74e3

12-PWR 1534.00 1355.40 1.20e3

5-DHLW 2314.00 2135.40 1.86e3

44-BWR 1878.00 1699.40 1.49e3

21-PWR 1858.00 1679.40 1.47e3

THIS DRAWING IS PRELIMINARY AND NOT INTENDED FOR CONSTRUCTION, PROCUREMENT, OR FABRICATION.

ANALYSES & COMPONENT DESIGN
Bechtel SAIC Company, LLC
SKETCH NUMBER ISK-0234
REVISION 01
SCALE AS NOTED SHEET 5 OF 5